THE GFAP.HMOX1 MOUSE MODEL OF PARKINSON DISEASE – microRNA, mRNA AND PROTEIN EXPRESSION PROFILES

by

MARISA CRESSATTI

B.Sc., University of Guelph, 2012

A THESIS SUBMITTED IN PARTIAL FULFILMENT OF THE REQUIREMENTS OF THE DEGREE OF

MASTER OF SCIENCE

in

THE FACULTY OF MEDICINE

(Integrated Program in Neuroscience)

MCGILL UNIVERSITY

(Montreal)

June 2016

ABSTRACT

Idiopathic Parkinson's disease (PD) is a movement disorder of unknown etiology characterized by the accelerated loss of dopaminergic (DA) neurons and accumulation of alpha-synuclein in the pars compacta of the substantia nigra (SN) and striatum (STM) brain regions. In recent years, Dr. Hyman Schipper's laboratory has engineered a novel parkinsonian GFAP.HMOX1$^{8.5\text{-}19m}$ mouse model, in which glial heme oxygenase-1 (HO-1), a stress protein induced in the PD SN, is overexpressed in the astroglial compartment. This model recapitulates many neurochemical, neuropathological and behavioural features of the disease. The objective of the current study was to further characterize the GFAP.HMOX1 mice through a broad genetic screen, evaluating key genes involved in various pathways that have been implicated in PD pathogenesis. MicroRNA (miRNA), messenger RNA (mRNA) and protein expression levels were analyzed both *in vivo* and *in vitro*. GFAP.HMOX1 neural tissues exhibited altered patterns of miRNA and target mRNA expression akin to those observed in human PD subjects. Several genes involved in the DA system were significantly downregulated, including dopamine transporter (DAT), tyrosine hydroxylase (TH), Nurr1, Pitx3 and LMX1B, at the mRNA and/or protein level in transgenic (TG) SN and STM compared to wild-type (WT) controls, while select miRNAs targeting these genes were significantly upregulated. Alpha-synuclein, involved in the formation of Lewy bodies in PD subjects, was significantly upregulated at both the mRNA and protein level in both brain regions, while several miRNAs targeting alpha-synuclein were significantly downregulated. Genes involved in other pathways known or suspected to play a role in PD pathology, such as oxidative stress, apoptosis, autophagy and mitophagy, mitochondrial

biogenesis and reelin regulation were significantly elevated at the mRNA and/or protein level in the experimental samples compared to WT preparations. Many of these whole-brain findings were recapitulated in neurons co-cultured with TG astrocytes compared to WT controls. Overexpression of astrocytic *HMOX1* in mice between 8.5 and 19 months of age promotes several behavioural, neurochemical, neuropathological and regulatory features of idiopathic PD. Curtailment of glial HO-1 hyperactivity by pharmacological or other means may afford neuroprotection in PD and other aging-related neurodegenerative disorders.

RÉSUMÉ

La maladie idiopathique de Parkinson (PD) est une maladie du mouvement d'étiologie inconnue caractérisée par la perte accélérée des neurones dopaminergiques (DA) et de l'accumulation de la protéine alpha-synucléine dans la pars compacta de la substance noire (SN) et le striatum (STM) du cerveau. Au cours des dernières années, le laboratoire de Dr. Hyman Schipper a conçu un modèle parkinsonien de souris GFAP.HMOX1$^{8.5\text{-}19m}$, où l'hème oxygénase-1 (HO-1) gliale, une protéine de stress induite dans le PD SN, est surexprimée dans les astrocytes. Ce modèle récapitule de nombreux aspects neurochimiques, neuropathologiques et comportementaux de la maladie de Parkinson. L'objectif de ma thèse était de caractériser les souris GFAP.HMOX1$^{8.5\text{-}19m}$ en utilisant un criblage génétique large pour identifier des gènes clés impliqués dans la pathogenèse de la maladie de Parkinson. Les micro ARN (miARN), ARN messagers (ARNm) et les niveaux d'expression de protéines cibles ont été analysés à la fois *in vivo* et *in vitro*. Nos résultats montrent que la transcription de certains miARN et ARNm qui est perturbée chez des sujets parkinsoniens humains est également perturbée dans les tissus neuraux des souris GFAP.HMOX1$^{8.5\text{-}19m}$. En particulier, la transcription et/ou l'expression de plusieurs gènes ou protéines impliqués dans le système DA est significativement diminuée dans le SN et le STM des souris transgénique comparés aux souris contrôles, y compris-le transporteur de la DA, la tyrosine hydroxylase, Nurr1, Pitx3 et LMX1B, tandis que certains miARN ciblant ces gènes sont significativement surexprimés. L'ARNm et la protéine alpha-synucléine qui est impliquée dans la formation des corps de Lewy chez les sujets PD sont aussi accrus dans les deux régions du cerveau des souris transgéniques, tandis que plusieurs

miARN ciblant l'alpha-synucléine sont réduits. Les gènes impliqués dans d'autres voies connues ou soupçonnées de jouer un rôle dans la pathologie PD sont aussi plus transcrits chez les animaux transgéniques, en particulier ceux impliqués dans le stress oxydatif, l'apoptose, l'autophagie et la mitophagie, la biogenèse mitochondriale et la régulation de reelin. Un grand nombre de ces découvertes observations ont été confirmées dans les neurones en co-culture avec des astrocytes transgéniques par rapport aux contrôles. En résumé, la surexpression de *HMOX1* gliale chez la souris entre 8.5 et 19 mois d'âge favorise plusieurs caractéristiques comportementales, neurochimiques, neuropathologiques et régulatrice de la maladie de Parkinson. L'interruption de l'hyperactivité de HO-1 gliale par des moyens pharmacologiques ou autres pourrait avoir un effet de neuroprotection dans PD et d'autres troubles neurodégénératifs liés au vieillissement.

ACKNOWLEDGEMENTS

I would like to thank my supervisor, Dr. Hyman Schipper, for giving me the opportunity to join his research team. Dr. Schipper has been incredibly supportive throughout the course of my M.Sc. Thesis work. I would also like to thank my committee members, Dr. Edward Fon and Dr. Kostantinos Pantopoulos, and my mentor, Dr. Heidi McBride, for their advice and input on the project. I have been fortunate enough to be able to work with a great team of researchers in the Schipper lab. I could not have completed this work without their support and guidance, most notably Dr. Wei Song. Dr. Song has offered a tremendous amount of help throughout this project, for which I am extremely grateful. I would also like to appreciate Adrienne Liberman, Carmela Galindez, Ayda Tavitian, Irene Yacoub and Dr. Mervyn Gornitsky. Several volunteer students have also generously contributed their time and effort to this research project, namely Jessica Hier, Elka Schwartz and Julia Galindez.

Lastly, I would like to thank my friends and family for their continued support in everything I do.

PREFACE AND CONTRIBUTION OF AUTHORS

During my M.Sc. Thesis research project, I was included as a co-author in two major works. The first publication: Lin SH, Song W, Cressatti M, Zukor H, Wang E, and Schipper HM (2015) Heme Oxygenase-1 Modulates microRNA Expression in Cultured Astroglia: Implications for Chronic Brain Disorders. GLIA 63: 1270-1284. I am *third author* of this manuscript and contributed to the identification of putative mRNA targets of the altered microRNA. I also contributed with editing of the manuscript. The second manuscript will be submitted for publication to the American Journal of Clinical Nutrition, entitled “Cysteine-Rich Whey Protein Isolate (Immunocal®) Ameliorates Deficits in the GFAP.HMOX1 Mouse Model of Schizophrenia.” I am *third author* of this manuscript and contributed with experimental guidance, writing and editing.

LIST OF TABLES

LIST OF FIGURES

LIST OF ABBREVIATIONS

6-OHDA: 6-Hydroxydopamine
AADC: Aromatic L-amino acid decarboxylase
AD: Alzheimer's disease
Ago2: Argonaute-2
Ara-C: Arabinose C
Bach1: Basic leucine zipper transcription factor 1
BAK (Bak1): Bcl-2 homologous antagonist killer
Bax: Bcl-2 associated X protein
Bcl-2: B cell lymphoma 2
BECN1: Beclin-1
CCAC: Canadian Council on Animal Care
CNS: Central nervous system
CO: Carbon monoxide
CO_2: Carbon dioxide
COMT: Catechol-O-methyl transferase
Crmp1 (Drp1): Collapsin response mediator protein1
CtsB: Cathepsin B
CtsD: Cathepsin D
DA: Dopamine
DAT: Dopamine transporter
FACS: Fluorescence-activated cell sorting
Fbw7: F-boc/WD repeat-containing protein 7
FITC: Fluorescein
GABA: gamma-Aminobutyric acid
GAD1 (GAD67): Glutamate decarboxylase
GAPDH: Glyceraldehyde 3-phosphate dehrydrogenase
GFAP: Glial fibrillary acidic protein
GPe: External globus pallidus
GPi: Internal globus pallidus
Hdac6: Histone deacetylase 6
HNE: 4-Hydroxy-2-nonenal
HO: Heme oxygenase
HVA: Homovanillic acid
L-DOPA: L-3,4-dihydroxyphenylalanine
Lamp2: Lysosomal-associated membrane protein 2
LDHA: Lactate dehydrogenase A
LMX1B: LIM homeobox transcription factor 1, beta
LRRK2: Leucine-rich repeat kinase 2
mAb: Monoclonal antibody
MAO: Monoamine oxidase
MARE: Maf recognition element
Mfn1: Mitofusin-1
Mfn2: Mitofusin-2
miRNA: MicroRNA
MPTP: 1-methyl-4-phenyl-1,2,3,6-tetrahydropyridine
mRNA: Messenger RNA
Notch1: Notch homolog 1, translocation-associated (Drosphilia)
Nrf2: Nuclear factor (erythroid-derived 2)-like 2
Nurr1 (Nr4a2): Nuclear receptor related-1 protein
OPA-1: Optic atrophy 1
P1: Postnatal day 1
p21 (CDKN1A): Cyclin-dependent kinase inhibitor 1A
p53 (TP53): Tumor protein p53
p62 (Nup62): Nucleoporin62
pAb: Polyclonal antibody
Park2 (PRKN): Parkin RBR E3 ubiquitin protein ligase
Park7 (DJ-1): Parkinson disease protein 7
PARP1: Poly (ADP-Ribose) polymerase 1
PD: Parkinson disease
PGC1-α (Ppargc1a): Peroxisome proliferator-activated receptor gamma, coactivator 1 alpha
PI: Phosphatidyl inositol
PINK1: PTEN-induced putative kinase 1
Pitx3: Pituitary homeobox 3
PTEN: Phosphatase and tensin homolog
PUMA (BBC3): BCL2 binding component 3
Reln (Reeler): Reelin
REM: Rapid eye movement
RISC: RNA-induced silencing complex
ROS: Reactive oxygen species
SEM: Standard error of the mean
Sirt1: Sirtuin 1
Smad3: Mothers against decapentaplegic homolog 3
SN: Substantia nigra
SNCA: alpha-synuclein
SnMP: Tin mesoporphyrin
SOD2 (MnSOD): Superoxide dismutase 2, mitochondrial
STM: Striatum
STN: Subthalamic nucleus
TEM: Transmission electron microscopy
TG: Transgenic
TGF-1β: Transforming growth factor beta 1
TH: Tyrosine hydroxylase
TRE: Tetracycline response element
tTA: Tetracycline transactivator
Uba52: Ubiquitin A-52 residue ribosomal protein fusion product 1
UTR: Untranslated region
VMAT2: Vesicular monoamine transporter 2
VTA: Ventral tagmental area
WT: Wild type

INTRODUCTION

Given an aging population that is both growing larger and living longer, neurodegenerative disorders are becoming increasingly prevalent in the developed world. Idiopathic Parkinson disease (PD) is a movement disorder of uncertain etiology that afflicts 1-2% of the population over 65 years of age. This progressive neurodegenerative disorder was first described by James Parkinson, a physician, in 1817, in which he reported on six cases observed in the streets of London as having "involuntary tremulous motion, with lessened muscular power, in parts not in action and even when supported; with a propensity to bend the trunk forward, and to pass from a walking to a running pace" (Parkinson, 1817). Initially referred to as "shaking palsy" or "paralysis agitans," French neurologist Jean-Martin Charcot later coined the term "Parkinson's disease" in 1872, seeing as not all patients had tremor (Charcot, 1872). Today, PD is the second most common neurodegenerative disorder (after Alzheimer's disease (AD)) and the most common movement disorder among older adults. PD is characterized pathologically by progressive degeneration of dopaminergic (DA) neurons in the substantia nigra pars compacta (SN) and striatum (STM), formation of fibrillar inclusions (Lewy bodies) in this cell population and variable depletion of other bioaminergic neurotransmitter systems (Hornykiewicz, 1988). This results in a slew of motor, autonomic and cognitive disabilities in patients. Generally, the clinical and pathological features of PD are the same amongst idiopathic and familial PD, however there remain significant differences in the risk factors between the two (Lai et al., 2002). Idiopathic cases of PD are far more common than familial PD (Morris, 2005). Furthermore, there is a higher incidence and prevalence of PD in men, possibly due to

the neuroprotective effects of estrogen to the DA system in women (Samii et al., 2004; Smith and Dahodwala, 2014). Today, there is no effective treatment strategy that slows the destruction of nerve cells in the affected brain regions for this debilitating condition, making research in this field imperative.

Motor Symptoms of Parkinson's Disease

The most common motor abnormalities observed in PD patients include resting tremor, rigidity, postural instability, bradykinesia, akinesia, shuffling gait and freezing. Motor symptoms manifest in PD subjects only after approximately 80% striatal DA loss and 60% loss of SN neurons (Kish et al., 1988; Morris et al., 1988; Fearnley and Lees, 1991). Typically, tremor is the first motor symptom to appear in patients (Hughes et al., 1993; Jankovic, 2008). Muscle rigidity, described as increased resistance to passive joint movement, can often lead to a flexed posture. Bradykinesia, described as extreme difficulties with planning, initiating and executing movements, as well as with performing sequential and simultaneous tasks, is a hallmark of basal ganglia disorders, such as PD (Berardelli et al., 2001). This often results in deficits in fine motor control, slower reaction times and general slowness of performing daily activities. Furthermore, akinesia in PD patients leads to loss or impairment of the power of voluntary movement. The combination of the above mentioned motor symptoms, in addition to poor balance, shuffling gait and freezing, ultimately leads to a higher incidence of falls amongst PD patients and hence greater disability. In addition to these motor abnormalities, cognitive and autonomic impairments are also prevalent in PD patients.

Non-Motor Symptoms of Parkinson's Disease

PD is a multi-system disease that affects a variety of brain structures at different time points along the course of manifestation, hence both motor and non-motor symptoms are observed (Kalia and Lang, 2015). Non-motor symptoms include olfactory dysfunction, sleep perturbations, autonomic dysfunction, gastrointestinal distress, memory loss and dementia, depression and anxiety, among others (Kalia and Lang, 2015). One of the most common non-motor symptoms is olfactory dysfunction, occurring in approximately 90% of PD patients (Hawkes et al., 1997). Sleep disturbances are also commonly observed in PD patients, manifesting as obstructive sleep apnea, restless legs syndrome, periodic limb movement syndrome and rapid eye movement (REM) sleep behaviour disorder (Tandberg et al., 1998; Neikrug et al., 2013). Dysphagia (difficulty swallowing), esophageal dysmotility (irregular contractions of the esophagus), constipation and hypotension are some common symptoms relating to autonomic dysfunction in this disease (Jost, 1997). Depression is prevalent in 36-50% of PD patients, in addition to anxiety, panic attacks, loss of initiative and assertiveness, anhedonia and fatigue (Shulman et al., 2001). Finally, late stage PD often leads to greater cognitive dysfunction, dementia and significant memory loss. However, many of the non-motor symptoms precede the occurrence of motor symptoms in PD, including olfactory dysfunction, REM sleep behaviour disorder, constipation, excessive daytime somnolence, symptomatic hypotension, erectile dysfunction, urinary dysfunction and depression, opening the avenues in search of potential preclinical biomarkers of PD (Schenck et al., 1996; Abbott et al., 2003; Chaudhuri et al., 2006; Siderowf et al., 2007).

Current Treatment Strategies

Current treatment strategies to treat PD remain purely symptomatic, with nothing on the market that significantly slows or prevents the degeneration of DA in affected brain regions. The most commonly prescribed treatment of PD is a pharmacological regimen based on DA replacement with the pro-drug, levodopa (L-3,4-dihydroxyphenylalanine; L-DOPA), in combination with an inhibitor of its peripheral conversion to DA, carbidopa, together called Sinemet (Brichta et al., 2013). Inhibitors of the enzymes involved in DA breakdown, such as monamine oxidase B (MAO-B), called selegiline and rasagiline, or catechol-O-methyltransferase (COMT), called entacapone and tolcapone, can be prescribed in combination with Sinemet in order to prolong its effects via blocking of L-DOPA metabolism (Kalia and Lang, 2015). Other therapies also exist, including DA agonists, namely pramipexole or ropinirole, which are less likely to cause drug-related dyskinesia, or anticholinergics, which mainly treat tremor and dystonia (Kalia and Lang, 2015). This high pill-burden treatment program is accompanied by a host of adverse effects, including motor response fluctuations, drug-related dyskinesia, nausea, vomiting, low blood pressure, hallucinations and psychosis (Kalia and Lang, 2015).

The Dopaminergic System in Parkinson's Disease

DA is a catecholamine neurotransmitter involved in cognition, learning and memory, reward, addiction, stress and movement (Beninger, 1983). DA neurons predominate in the ventral tegmental area (VTA) and SN of the midbrain, as well as the arcuate nucleus of the hypothalamus (Beninger, 1983). Intracellular DA metabolism begins with the conversion of the amino acid tyrosine into L-DOPA by the rate-limiting

enzyme tyrosine hydroxylase (TH) (Meiser et al., 2013). L-DOPA is subsequently decarboxylated into DA by aromatic acid decarboxylase (AADC). At this point, DA enters pre-synaptic vesicles via vesicular monoamine transporter type 2 (VMAT2), followed by the release of vesicles into the extracellular synaptic space (Meiser et al., 2013). Extracellular DA is either converted by COMT and MAO-B into homovanillic acid (HVA) or extracellular DA is transported back into the pre-synaptic terminal via dopamine transporter (DAT). Upon uptake, DA is converted by MAO-A into DOPAC, which is then converted into HVA via COMT (Meiser et al., 2013). The interaction between DA and post-synaptic receptors is essential in the modulation of motor function through circuitry interconnecting the basal ganglia, thalamus and motor cortex.

This modulation of motor function, or the initiation normal and abnormal motor behaviour, is classically described by the basal ganglia model (Penney and Young, 1986; Crossman, 1987; Albin et al., 1989; DeLong, 1990). The basal ganglia are composed of four interconnected nuclei: the caudate and putamen (STM), the internal and external portions of the globus pallidus (GPi; GPe), the SN (pars reticulata and pars compacta) and the subthalamic nucleus (STN). In order to mediate voluntary movement, maintenance of the equilibrium between two contrasting pathways originating in the STM, namely the direct and indirect pathways, is regulated by the SN pars compacta DA projection neurons that synapse with striatal gamma-aminobutyric acid (GABA) neurons (DeLong and Wichmann, 2007). The direct pathway begins with glutamatergic stimulation of the STM by the cerebral cortex, leading to inhibition of the SN pars reticulata and GPi complex via GABAergic projections and subsequent reduction in thalamus inhibition (DeLong and Wichmann, 2007). Thus, the thalamus is

able to stimulate the cortex to a greater extent, leading to increased muscle stimulation and a hyperkinetic state. The indirect pathway begins in the same way as the direct pathway, with glutamatergic stimulation of the STM by the cerebral cortex, however this leads to inhibition of the GPe via GABAergic projections, resulting in less inhibition of the STN (DeLong and Wichmann, 2007). The STN, the only portion of the basal ganglia with excitatory glutamatergic projections, stimulates the SN pars reticulata and GPi complex, ultimately leading to greater inhibition of the thalamus and less subsequent stimulation of the cortex (DeLong and Wichmann, 2007). The cortex is not able to stimulate the muscles as much, resulting in a hypokinetic state. This antagonistic relationship between the direct and indirect pathway is largely mediated by DA output from the SN pars compacta to the STM, in which DA acts to increase the excitatory effect of the direct pathway and decrease the inhibitory effect of the indirect pathway (DeLong and Wichmann, 2007).

Accelerated loss of DA neurons in the pars compacta of the SN is a hallmark of PD, in which the hypokinetic state is favoured due to decreases in DA and resultant over-activity of the indirect pathway (Hornykiewicz, 1988). Progressive DA loss in the midbrain affects different parts of the nigral complex to varying degrees, however the most severe degeneration is observed in the ventrolateral part of the SN (Hassler, 1938; Fearnley and Lees, 1991). While DA neurons compose less than 1% of the total number of neurons in the brain, their degeneration in PD results in profound motor, autonomic and cognitive disabilities. DA neurons are prone to oxidative stress due to the high rate of oxygen metabolism, low level of antioxidants and high iron content (Chinta and Anderson, 2005). Furthermore, DA oxidation via MAO generates hydrogen peroxide,

oxygen radicals, semiquinones and quinones, contributing to the elevated levels of oxidative stress in PD brain (Chinta and Anderson, 2005).

Alpha-Synuclein in Parkinson's Disease

Lewy bodies are primarily composed of alpha-synuclein, which has been found to accumulate widely in central and peripheral neurons of PD patients (Lansbury and Lashuel, 2006; Cookson and van der Brug, 2008; Winklhofer et al., 2008). This 14-kDa protein is localized to presynaptic terminals and portions of the nuclear envelope and plays a significant role in SNARE-mediated exocytosis and synaptic vesicle transport (Marques and Outeiro, 2012). Alpha-synuclein is present in mitochondria in PD brain and has been previously shown to affect mitochondrial function both *in vitro* and *in vivo*, ultimately contributing to the vulnerability of nigrostriatal DA neurons in PD (Devi et al., 2008; Nakmura et al., 2008; Shavali et al., 2008; Zhang et al., 2008; Subramaniam et al., 2014). While mechanisms of abnormal alpha-synuclein aggregation in neurodegenerative diseases are unclear, it has been previously shown that alpha-synuclein aggregation is closely related to oxidative reactions, which may play a critical role in neurodegeneration in disorders with Lewy bodies, like PD (Hashimoto et al., 1999).

Similar to prion proteins, it has been hypothesized that alpha-synuclein aggregates can cross the cell membrane and directly contribute to propagation of neurodegenerative disease pathology (Angot and Brundin, 2009; Kordower and Brundin, 2009; Angot et al., 2010; Frost and Diamond, 2010). Binding of native unfolded alpha-synuclein to membranes or vesicles containing acidic phospholipids leads to the alpha-helical conformation of alpha-synuclein. Dimerization of Tyr125 is the initial and

rate-limiting step that ultimately leads to a greater potential to self-interact (Chu and Kordower, 2015). This dimerized alpha-synuclein acts as the template for native alpha-synuclein monomers to refold into protofibrils. Oligomers and fibrils rich in beta-sheets comprise the pathological form of alpha-synuclein. This self-propagated conformational change is also highly characteristic of prion proteins. Furthermore, seeding fibrilar A30P alpha-synuclein to WT alpha-synuclein monomers results in fibrils similar to the mutant fibrils (Yonetani et al., 2009). Alpha-synuclein aggregation is thought to be the driving force of PD pathogenesis. This is supported by evidence from a transgenic mouse model of synucleinopathy (TgM83), whereby young asymptomatic mice with alpha-synuclein preformed fibrils, prepared from older symptomatic mice, resulted in accelerated alpha-synuclein hyperphosphorylation at Ser129 (the pathological form of alpha-synuclein that is predominantly found in Lewy bodies), aggregated alpha-synuclein and decreased survival time (Sacino et al., 2014).

Oxidative Stress in Parkinson's Disease

Oxidative stress is defined as a disequilibrium between the levels of reactive oxygen species (ROS) produced and the ability of a biological system to detoxify the reactive intermediates, ultimately creating a perilous state contributing to cellular damage (Dias et al., 2013). In PD, oxidative stress is thought to contribute to the degeneration of DA neurons in the SN and STM. Notably, DA metabolism itself is a primary source of ROS, as mentioned above, in addition to mitochondrial dysfunction, neuroinflammatory cells, calcium as well as aging. Iron also contributes to ROS production in PD, seeing as cellular iron storage mechanisms and antioxidant capacities are overwhelmed by misdistribution of iron and the ensuing oxidative damage in the

disease state (Devos et al., 2014). This is further supported by postmortem brain analyses showing increased levels of 4-hydroxyl-2-nonenal (HNE), a by-product of lipid peroxidation, carbonyl modifications of soluble proteins and DNA and RNA oxidation products 8-hydroxy-deoxyguanosine and 8-hydroxy-guanosine (Yoritaka et al., 1996; Alam et al., 1997; Floor and Wetzel, 1998; Zhang et al., 1999; Jenner, 2003). In PD, primary insults (endogenous or environmental) lead to oxidative stress, which damages mitochondria and key cellular proteins that, in turn, cause more ROS production (a feed forward, self-perpetuating system), eventually leading to neuronal degeneration (Dias et al., 2013).

Mitochondrial Dysfunction in Parkinson's Disease

Mitochondria are essential for proper cellular function, being responsible for cellular respiration, energy metabolism, calcium homeostasis, stress response and cell death pathways. Mitochondrial dysregulation plays a critical role in the pathogenesis of PD, particularly since mitochondria act as both a source and target of ROS. Decreased activity of complex I of the mitochondrial electron transport chain has been widely associated with PD (Schapira et al., 1989; Beal, 1995; Shults et al., 1997; Jenner, 2003; Keeney et al., 2006). Furthermore, PD-causing gene products, including DJ-1, PINK1, Parkin, alpha-synuclein and LRRK2, also impact mitochondrial function leading to exacerbation of ROS generation and increased susceptibility to oxidative damage (Dias et al., 2013). Autophagy of the mitochondria, otherwise known as mitophagy, involves some of these PD-causing gene products, namely DJ-1, PINK1 and Parkin, and is negatively impacted by oxidative stress (Dias et al., 2013).

Animal Models of Parkinson's Disease

Although interactions between environmental and genetic factors have been implicated as pathogenic mechanisms of selected neuronal degeneration, the etiology of PD remains unknown. Research on parkinsonian animal models has been employed in order to better understand the etiology, pathogenesis and molecular mechanisms underlying the disease process. The animal models most frequently studied in relation to PD include those generated by neurotoxic chemicals that selectively disrupt the catecholaminergic system such as 6-hydroxydopamine (6-OHDA) or 1-methyl-1,2,3,6-tetrahydropiridine (MPTP); agricultural pesticide toxins, such as rotenone and paraquat; the ubiquitin proteasome system inhibitors; inflammatory modulators; and several genetically manipulated models, such as mutant alpha-synuclein, Smad3, DJ-1, PINK1, Parkin, and LRRK2 transgenic (TG) or knock-out animals (Le et al., 2014). The neurotoxic models, most notably the MPTP primate model, appear to be best suited for testing therapeutic interventions aimed at counteracting motor symptoms of PD, however these models generally do not reproduce the progressive course of PD (Le et al., 2014). On the other hand, TG or knockout genetic models may better recapitulate the pathogenic mechanisms of genetic forms of PD, but their pathological and behavioural phenotype does not mimic human PD (Le and Jankovic, 2013; Le et al., 2014).

Smad3 is involved in the intracellular TGF-β1 signaling cascade, playing a role in the control of cell growth, proliferation and differentiation, as well as apoptosis. Smad3-deficient mice have proven a useful model of PD, displaying selective postnatal neurodegeneration of DA midbrain neurons, strong MAO-mediated catabolism of DA in

STM, oxidative stress and dampening of trophic and astrocytic support to DA neurons (Tapia-Gonzalez et al., 2011). Moreover, Smad3-deficient mice also possess Ser129-phosphorylated-alpha-synuclein inclusions extensively in the perikaryon and neurites of specific brain nuclei (Tapia-Gonzalez et al., 2011).

However, many of the current parkinsonian animal models fail to reproduce both hallmarks in PD pathology. Mice with TG expression of human autosomal dominant mutants of alpha-synuclein or the LRRK2 do not display overt midbrain DA neurodegeneration (Li et al., 2009; Westerlund et al., 2010; Bifsha et al., 2014). Murine loss-of-function mutations in autosomal recessive gene products for PINK1 and Parkin have not been illuminating in this regard either, with the exception of DJ-1 (Bifsha et al., 2014; Rousseaux et al., 2012). The novel GFAP.HMOX1 TG mouse model of PD, recently engineered to allow conditional and selective expression of *HMOX1*, by the astrocytic compartment, displays reduced striatal DA and increased alpha-synuclein immunoreactivity, among other pathological and behavioural hallmarks of PD (see below).

Heme Oxygenase-1

Over the past two decades, the Schipper laboratory has adduced considerable evidence implicating the stress-inducible enzyme, heme oxygenase-1 (HO-1), in the pathogenesis of PD. Two forms of HO exist in the human body, namely HO-1 and HO-2. Both enzymes exhibit identical substrate and cofactor specificities, however distinct genes encode each isoform and they share only 43% sequence homology in humans (Dennery, 2000; Loboda et al., 2008). Moreover, HO-1 and HO-2 exhibit significant differences in molecular weight, electrophoretic mobility, antigenicity, cellular distribution

and regulation. While HO-2 expression is constitutive, abundant and fairly ubiquitous, HO-1 is minimally expressed and confined to scattered neuroglia and sparse populations of neurons in the brain (Vincent et al., 1994; Matz et al., 1996; Bergeron et al., 1998). Furthermore, unlike HO-2, HO-1 is readily inducible by a number of factors, including heme, hypoxia, oxidative stress, Th1 cytokines, thiol-reactive substances, sulfhydryl agents, nitric oxide, heavy metals and ultraviolet irradiation (Dennery, 2000; Schipper, 2000; Kinobe et al., 2006; Loboda et al., 2008). Control mechanisms for HO-1 induction and homeostasis in stressed brain and other organs involve Nrf2 transcription factor binding to Maf response elements (MARE) in *HMOX1* promoter and repression of the gene by the heme-regulated protein, Bach1 (Ogawa, 2002; Sun et al., 2002; Kitamuro et al., 2003; Suzuki et al., 2003;). The current research project focuses primarily on the roles of HO-1 in brain aging and PD.

HO-1 resides in the endoplasmic reticulum where it catalyzes the conversion of heme to biliverdin, which is subsequently converted to bilirubin by biliverdin reductase, in addition to releasing equimolar amounts of carbon monoxide (CO) and free ferrous iron (Figure 1). NADPH is required as an electron donor in both enzymatic reactions catalyzed by HO-1 and biliverdin reductase. While biliverdin and bilirubin have antioxidant properties, CO and free ferrous iron may promote cellular injury by the production of free radicals within mitochondrial and other cellular compartments, leading to oxidative stress, mitochondrial dysfunction and increased levels of unregulated iron (Schipper et al., 1998). The latter comprise a ‘core’ neuropathology common to PD and other aging-related neurodegenerative disorders (Schipper, 2004).

Heme Degradation Products

The dual-nature of HO-1 is largely attributed to the heme degradation reaction products. Biliverdin and bilirubin are cellular antioxidants capable of scavenging peroxyl radicals, inhibiting lipid peroxidation and protecting cells from excess hydrogen peroxide. However, excessive and prolonged hyperbilirubinemia of untreated neonatal jaundice may incur irreversible neurological injury, called kernicterus (Qato and Maines, 1985). While CO promotes intracellular free radical generation under certain circumstances; it can also act as a neurotransmitter, playing a role in the modulation of inflammatory response, vasodilation, neurovascular growth and inhibition of blood platelet aggregation and adhesion. Even free ferrous iron, which readily partakes in Fenton chemistry, leading to the production of hydroxyl radicals and thus protein oxidation, lipid membrane peroxidation and nucleic acid mutagenesis, possesses protective properties through cellular detoxification. The Janus-faced behaviour of HO-1 highlights the importance of the intensity and chronicity of human HO-1 gene, *HMOX1*, induction, the cell type of origin and the chemistry of the local redox microenvironment in determining whether the antioxidant benefits of a diminished heme:bilirubin ratio or oxidative damage accruing from intracellular mobilization of iron/CO predominates.

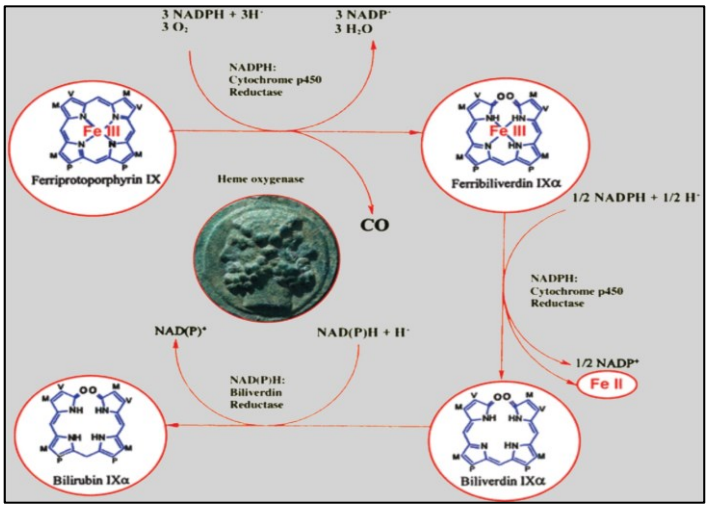

Figure 1. Heme oxidation mediated by heme oxygenase. Modified from Ryter and Tyrrell, 2000.

Heme Oxygenase-1 in Disease

Constitutive expression of this stress protein is very low in the course of normal brain aging, however HO-1 overexpression has been documented in a number of disease states other than PD (Ewing et al., 1992). In AD brains, numerous neurons throughout the hippocampus (pyramidal and dentate gyrus granule cells) and temporal cortex (layers II – V) exhibit intense, cytoplasmic HO-1 immunoreactivity (Schipper et al., 1995). Dual labeling for HO-1 and the astrocyte marker, glial acidic fibrillary protein (GFAP), revealed co-expression of HO-1 in 86% of GFAP-positive astrocytes in AD hippocampus compared to only 6.8% HO-1 co-expression with GFAP-positive astrocytes in the hippocampus of age-matched, non-demented controls (Schipper et al., 1995). Conversely, glial HO-1 immunoreactivty was minimal and not significantly different from control values in AD SN, a region largely spared by the disease (Schipper et al., 1995). Similarly, immunoreactive HO-1 was co-expressed in 57.3% of GFAP-positive astrocytes in spinal cord plaques procured postmortem from multiple sclerosis patients, compared to only 15.4% HO-1 co-expression with GFAP-positive astrocytes in

the spinal white matter of normal subjects (Mehindate et al., 2001). Furthermore, immunoreactive HO-1 protein has been shown to colocalize to neurofibrillary tangles in patients with progressive supranuclear palsy, Pick bodies in cases of frontotemporal dementia and ballooned neurons in corticobasal ganglionic degeneration (Castellani et al., 1995). The upregulation of HO-1 mRNA and protein in the central nervous system (CNS) and other tissues is widely accepted as a phylogenetically conserved, highly sensitive and reliable marker of oxidative stress (Schipper, 2007). The enhanced expression of glial HO-1 may contribute to the pathological deposition of non-transferrin iron and bioenergetic failures that have been repeatedly documented in the normal aging CNS and, to a much greater extent, in a broad range of human neurodegenerative and neuroinflammatory disorders.

Considering the dual effects of HO-1, it is interesting to note that in a recent study looking at an autologous blood injection intracerebral hemorrhage model, selective HO-1 overexpression in astrocytes actually had a protective role, ultimately reducing mortality, blood-brain barrier disruption, perihematomal cell injury and neurological deficits (Chen-Roetling et al., 2015). While prolonged glial HO-1 overexpression results in a pro-oxidant effect, acute increase of astrocytic HO-1 may actually lead to beneficial antioxidant effects via the heme degradation pathway products, biliverdin and bilirubin, particularly in the case of intracerebral hemorrhage (Chen-Roetling et al., 2015).

Heme Oxygenase-1 in Parkinson's Disease

The fraction of GFAP-positive astrocytes concomitantly expressing HO-1 in *post mortem* PD SN was 77.1%, significantly greater than the 18.7% observed in the SN of

control subjects (Schipper et al., 1998). Moreover, HO-1 immunoreactivity in DA (neuromelanin-containing) neurons of the PD SN revealed that Lewy bodies in these cells consistently manifest intense HO-1 staining in their peripheries (Schipper et al., 1998). Transfection of the *HMOX1* in cultured rat astroglia results in dystrophic mitochondria, increased iron deposition and evidence of macroautophagy compared to untreated and sham-transfected astrocytes (Zukor et al., 2009). The addition of tin mesoporphyrin (SnMP), a competitive inhibitor of HO, to the *HMOX1*-transfected astrocytes obviates these cytopathological changes (Zukor et al., 2009).

The GFAP.HMOX1$^{8.5\text{-}19m}$ Mouse Model

The Schipper laboratory has recently engineered a novel GFAP.HMOX1 TG mouse model to allow conditional and selective expression of *HMOX1* by the astrocytic compartment (Song et al., 2012). The tetracycline (Tet)-controllable ("Off") system permits temporal control of transgene expression at specific time points in the lifespan of the mouse (Figure 2). Interestingly, overexpression of HO-1 in astrocytes of GFAP.HMOX1 mice throughout embryogenesis until 12 months of age (GFAP.HMOX1$^{0\text{-}12m}$ model) resulted in a neuropathological and behavioural profile that bears resemblances to human schizophrenia and other neurodevelopmental conditions (Song et al., 2012). This is consistent with *HMOX1* induction observed in the prefrontal cortex of humans with schizophrenia (Prabakaran et al., 2004). In the parkinsonian GFAP.HMOX1$^{8.5\text{-}19m}$ mouse model, transgene expression is initiated at midlife, at approximately 8.5 months, until testing and sacrifice at approximately 19 months of age.

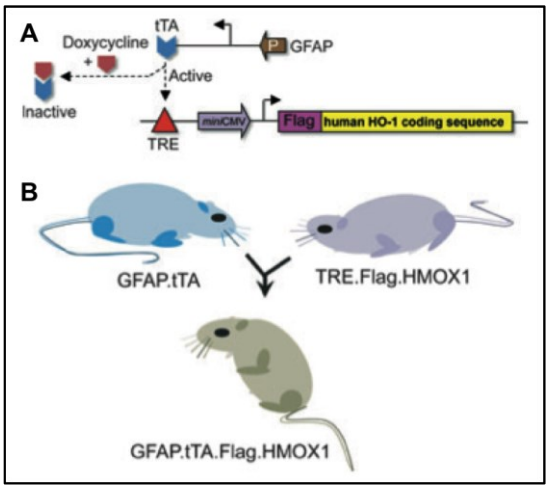

Figure 2. Construction of GFAP.HMOX1 transgenic mice. Modified from Song et al., 2012.

Unpublished transmission electron microscopy (TEM) data of astrocytes from the STM of a 19-month old GFAP.HMOX1$^{8.5\text{-}19m}$ mouse showed dystrophic mitochondria, increased iron deposition and evidence of macroautophagy compared to that of an age-matched, wild-type (WT) control animal. Additional unpublished neurochemistry measurements on TG mice at 19 months of age revealed significantly decreased DA in the STM ($p < 0.001$). Glial expression of the *HMOX1* transgene between 8.5 and 19 months of age also resulted in poor Rotarod performance, an index of locomotor coordination and balance. Moreover, a trend towards impaired motor coordination in mice expressing the transgene for an identical duration (10.5 months), but spanning the period from 1.5 to 12 months of age, did not achieve statistical significance, attesting to the importance of brain aging in symptom manifestation (data not published).

In addition to the 'core' neuropathology observed in PD patients as well as the GFAP.HMOX1$^{8.5\text{-}19m}$ mice, other commonly observed neuropathologies include decreased developmental and functional DA processes, increased protein aggregation (alpha-synuclein), increased apoptosis, autophagic and mitophagic dysfunction and

mitochondrial biogenesis imbalance. An extensive look at these features in the aging GFAP.HMOX1$^{8.5\text{-}19m}$ mouse model of PD will be the focus of this study, using a variety of *in vivo* and *in vitro* experimental techniques at the level of microRNA (miRNA), messenger RNA (mRNA) and protein expression.

MicroRNAs

MiRNAs are noncoding RNA species, 20-25 nucleotides in length, which bind to the 3' untranslated region (3'-UTR) of target genes (Bartel, 2004). Full complementarity between this post-transcriptional gene regulatory molecule and its target mRNA results in targeted mRNA cleavage, while partial complementarity causes targeted mRNA degradation and protein translation repression. Recent evidence suggests that dysregulated miRNA expression may play a pivotal role in developmental brain disorders, aging and neurodegenerative conditions (Kim et al., 2007; Lukiw, 2007; Boissonneault et al., 2009; Sethi and Lukiw, 2009). Many miRNAs target oxidative stress-responsive genes, such as the superoxide dismutases (SODs), as well as other gene families regulating cell survival and death, including those coding for heat shock proteins, apoptosis, trophic factors, DNA repair enzymes and cellular bioenergetics (Schipper et al., 2007).

The Schipper laboratory recently employed miRNA microchip assays on *HMOX1*- and sham-transfected primary rat astroglia in order to determine whether altered patterns of miRNA expression participate in *HMOX1*-related neural injury (Lin et al., 2015). This study concluded that altered expression profiles of salient miRNAs and their mRNA targets in chronic CNS disorders contribute to the neural damage accruing from the over-expression of glial HO-1. In *HMOX1*-transfected astrocytes, rno-miR-

140*, rno-miR-17 and rno-miR-16 were significantly upregulated, while rno-miR-297, rno-miR-206, rno-miR-187, rno-miR-181a, rno-miR-138 and rno-miR-29c were significantly downregulated, compared to sham-transfected controls (Lin et al., 2015). Furthermore, the heme degradation byproducts ferrous iron and CO were implicated in the *HMOX1* effects, whereas bilirubin was inert or counteracted the *HMOX1*-related changes (Lin et al., 2015). Alterations in the expression profiles of these miRNAs have been previously correlated with increased oxidative stress, mitochondrial dysfunction, macroautophagy and free iron deposition (Lin et al., 2015). These altered miRNAs, among others, and their predicted mRNA/protein targets will be part of the focus of this study.

Project Aims

1) To quantify levels of mRNAs and related miRNAs implicated in the pathogenesis of parkinsonism in aging GFAP.HMOX1 mice.

2) To employ primary astrocyte-neuronal co-cultures to delineate the impact of glial HMOX1 induction on neuronal gene expression and morphology.

3) To quantify expression levels of key proteins implicated in the pathogenesis of PD in GFAP.HMOX1 mice.

A successful outcome of the proposed experiments would further support glial HO-1 hyperactivity as a pivotal transducer that funnels an array of noxious stimuli through limited neurodegenerative pathways culminating in nigrostriatal injury. Positive results would underscore HO-1 as a potent driver of relevant cellular pathology and a potential therapeutic target in human PD. Furthermore, alterations in key miRNA expression levels could be used as a suitable preclinical biomarker for PD, considering

the stable nature of miRNAs and detectability in human plasma, serum or total blood, as well as urine and saliva.

MATERIALS AND METHODS

Animal Husbandry – The Animal Care Committee of McGill University, in accordance with the guidelines of the Canadian Council on Animal Care (CCAC), has approved all experimental protocols pertaining to the use of mice in this study. All mice were bred and cared for in the Animal Care Facilities at the Lady Davis Institute for Medical Research. Mice were kept at a room temperature of 21 ± 1°C with a 12 h light/dark schedule. As indices of general health, fur texture, body weight and survival rates were monitored. The mice used were of either sex.

Surgical Procedures – All mouse brains were fixed by transcardial perfusion at 19 months of age as previously described (Fenton et al., 1998). The brains were removed and frozen in dry ice immediately with 200 ml of ice-cold PBS and stored at -80°C.

PCR Genotyping – Crude extracts containing genomic DNA from tail biopsy specimens were recovered using the REDExtract-N-Amp Tissue PCR kit (Sigma-Aldrich). The tetracycline transactivator (tTA) coding sequence (1.009 kb fragment) was amplified with the primer pair (Forward: 5'-CGG CTC ATG ATG TCT AGA TTA GA-3'; Reverse: 5'-AAT TAG AAT TCT CGC GCC CCC TA-3'). The *Flag* + *HMOX1* gene segment (989 bp fragment) was amplified with tetracycline response element (TRE) sequence primer (Forward: 5'-CGC TGA GGA TCC ATG GAC TAC AAA GAC GAT-3'; Reverse: 5'-CGT GCA TCT AGA TCA CAT GGC ATA AAG CCC-3'). The primers used to amplify the glyceraldehyde 3-phosphate dehydrogenase (GAPDH) segment (385 bp fragment) were used as an internal control (Preisig-Muller et al., 1999). Amplifications were performed in a total volume of 20 µl containing 10 µl of REDExtract-N-Amp PCR

mix, 6 µl of a mixture of each primer and PCR grade water, plus 4 µl of the crude mouse tail extract as a template. The PCR protocol consisted of an initial step of 3 min at 94°C, followed by 35 cycles of 30 s at 94°C, 1 min at 57°C and 1 min at 72°C. The final extension cycle was 10 min at 72°C (Song et al., 2012).

Total RNA Extraction, Polyadenylation and cDNA Synthesis – Total RNA from each dissected brain region (SN and STM) or primary cell cultures was extracted in Trizol according to the manufacturer's instructions (Invitrogen). MiRNA polyadenylation was performed followed by cDNA synthesis using 2.5 µg of polyadenylated total RNA with Mir-X^{TM} miRNA First-Strand Synthesis Kit (Clontech). Extraction of mRNA was performed using 2 µg of total RNA subjected to RT-qPCR using Transcriptor First-Strand cDNA Synthesis Kit (Roche Diagnostics) and anchored-oligo-dT_{18} or random hexamer primer, and the resulting cDNA was amplified by PCR (Song et al., 2009).

Quantitative Real-Time PCR – The Applied Biosystems 7500 Fast RT-qPCR System (Applied Biosystems by Life Technologies) was used to quantify miRNA and mRNA with SensiFast SYBR Lo-ROX kit according to manufacturer's instructions (FroggaBio). 25 ng of cDNA were quantified using the RT-qPCR Kit (Invitrogen) via RT-qPCR. The forward and universal/reverse primer sequences used to detect mRNA were either designed with Primer Express Software, version 3.0 (Applied Biosystems by Life Technologies), or obtained by AlphaDNA (Table 1). As an internal reference, snoRNA-202 miRNA and β-actin mRNA were probed (Table 1). Expression fold changes between groups were calculated using the ΔΔCt method relative to controls following normalization with levels of either snoRNA-202 miRNA or β-actin mRNA (Livak and

Schmittgen, 2001). For each miRNA and mRNA target, 5 WT and 5 TG mice were analyzed *in vivo* and 5 litters of WT mice and 5 litters of TG mice were analyzed *in vitro*.

Table 1. MiRNA sequences for RT-qPCR.

	Sequence (5' to 3')
snoRNA-202	agtacttttgaaccctttcca
mmu-miR-145	gtccagttttcccaggaatccct
mmu-miR-133b	tttggtccccttcaaccagcta
mmu-miR-7a	tggaagactagtgattttgttgt
mmu-miR-7b	tggaagacttgtgattttgttgt
mmu-miR-153	ttgcatagtcacaaaagtgatc
mmu-miR-223	tgtcagtttgtcaaatacccca
mmu-miR-140*	taccacagggtagaaccacgg
mmu-miR-17	caaagtgcttacagtgcaggtag
mmu-miR-16	tagcagcacgtaaatattggcg
mmu-miR-137-5p	acgggtattcttgggtggataat
mmu-miR-137-3p	ttattgcttaagaatacgcgtag
mmu-miR-128-3p	tcacagtgaaccggtctcttt
mmu-miR-128-5p	cggggccgtagcactgtctga
mmu-miR-208a-3p	acaagctttttgctcgtcttat
mmu-miR-208b	acaaacctttgttcgtcttat
mmu-miR-200c-3p	taatactgccgggtaatgatgga
mmu-miR-34a-5p	acaaccagctaagacactgcca
mmu-miR-206	tggaatgtaaggaagtgtgtgg
mmu-miR-29c	tagcaccatttgaaatcggtta
mmu-miR181a	aacattcaacgctgtcggtgagt
mmu-miR-138	agctggtgttgtgaatcaggccg
mmu-miR-325	ttgataggaggtgctcaataaa

Table 2. mRNA sequences for RT-qPCR. F, forward primer; R, reverse primer.

	Sequence (5' to 3')
Bak (Bcl-2 homologous antagonist killer)	F: GGAATGCCTACGAACTCTTCACC; R: CAAACCACGCTGGTAGACGTAC
Bax (Bcl2-associated X protein)	F: AGGATGCGTCCACCAAGAAGCT; R: TCCGTGTCCACGTCAGCAATCA
Bcl2 (B cell lymphoma 2)	F: GGGATGCCTTTGTGGAACTATATG; R: CAGCCAGGAGAAATCAAACAGA
BECN1 (Beclin 1)	F: GGACAAGCTCAAGAAAACCAATG; R: TGTCCGCTGTGCCAGATGT
CtsB (Cathepsin B)	F: AGTCAACGTGGAGGTGTCTGCT; R: GTAGACTCCACCTGAAACCAGG
CtsD (Cathepsin D)	F: TAAGACCACGGAGCCAGTGTCA; R: CCACAGGTTAGAGGAGCCAGTA
DAT (Dopamine transporter)	F: GGTGCTGATTGCCTTCTCCAGT; R: GACAACGAAGCCAGAGGAGAAG
DJ-1 (Park7)	F: ACGATGTGGTGGTTCTTCCAGG; R: CTGCACAGATGGCAGCTATGAG
Drp1 (Dynamin-related protein)	F: GCGAACCTTAGAATCTGTGGACC; R: CAGGCACAAATAAAGCAGGACGG
GAD67 (Glutamic acid decarboxylase)	F: CGCTTGGCTTTGGAACCGACAA; R: GAATGCTCCGTAAACAGTCGTGC
Hdac6 (Histone deacetylase 6)	F: TCGCTGTCTCATCCTACCTGCT; R: GTCAAAGTTGGCACCTTCACGG
Lamp2 (Lysosome-associated membrane protein 2)	F: TGTGCCTCTCTCCGGTTAAAG; R: CGGCTCCTAGGAACAGAAAGATC
LMX1β (LIM homeobox transcription factor 1-β)	F: GAAGGAGAAAGACCTGCTCAGC; R: TCCACTGCCTTTACTCTGGCTG
Mfn1 (Mitofusion 1)	F: CCAGGTACAGATGTCACCACAG; R: TTGGAGAGCCGCTCATTCACCT
Mfn2 (Mitofusion 2)	F: GTGGAATACGCCAGTGAGAAGC; R: CACCTTGCTGGCACAGATGAGC
Notch1 (Notch homolog 1)	F: GCTGCCTCTTTGATGGCTTCGA; R: CACATTCGGCACTGTTACAGCC
Nurr1 (Nuclear receptor related-1 protein)	F: CCGCCGAAATCGTTGTCAGTAC; R: TTCGGCTTCGAGGGTAAACGAC
OPA-1 (Optic atrophy-1)	F: GCTCCTAGAAGACCTGATTCGC; R: AGGATTCGGCAAGTAAGCCTGG
p21 (Cyclin-dependent kinase inhibitor-1)	F: TCGCTGTCTTGCACTCTGGTGT; R: CCAATCTGCGCTTGGAGTGATAG
p53 (Tumor protein 53)	F: AACCGCCGACCTATCCTTAC; R: CTTCTGTACGGCGGTCTCTC
p62 (Nucleoporin)	F: GAGGAGCGTGAGAAGACCTACAA; R: ATGCGCTTGAGCTGAGCAT
Park2 (Parkin)	F: CCAGAGGAAAGTCACCTGCGAA; R: GTTCGAGCAGTGAGTCGCAATC
PARP1 (Poly[ADP-ribose] polymerase-1)	F: CCACGCACAACGCCTATG; R: CCCCCTCGCGCTCTATCT
PGC1α (Peroxisome proliferator-activated receptor gamma coactivator 1 α)	F: GAATCAAGCCACTACAGACACCG; R: CATCCCTCTTGAGCCTTTCGTG
PINK1 (PTEN-induced putative kinase 1)	F: CGACAACATCCTTGTGGAGTGG; R: CATTGCCACCACGCTACACT
Pitx3 (Pituitary homeobox 3)	F: CTTCCAGAGGAATCGCTACCCT; R: CTGCGAAGCCACCTTTGCACAG
PTEN (Phosphatase and tensin homolog)	F: TGAGTTCCCTCAGCCATTGCCT; R: GAGGTTTCCTCTGGTCCTGGTA
PUMA (p53 upregulated modulator of apoptosis)	F: ACCGCTCCACCTGCCGTCCGTCAC; R: ACGGGCGACTCTAAGTGCTGC
Reelin	F: GCCACGCCACAATGGAA; R: CGACCTCCACATGGTCCA
Sirt1 (Sirtuin-1)	F: CAGTGTCATGGTTCCTTTGC; R: CACCGAGGAACTACCTGAT
SNCA (α-synuclein)	F: CACTGGCTTTGTCAAGAAGGACC; R: CATAAGCCTCACTGCCAGGATC
SOD2 (Manganese superoxide dismutase)	F: TAACGCGCAGATCATGCAGCTG; R: AGGCTGAAGAGCGACCTGAGTT
TH (Tyrosine hydroxylase)	F: TGCACACAGTACATCCGTCATGC; R: GCAAATGTGCGGTCAGCCAACA
Uba52 (Ubiquitin A-52)	F: GCCAAGATCCAGGATAAGGAAGG; R: CCGAAGTCTCAACACCAGATGAA
β-actin	F: AGGGAAATCGTGCGTGAC; R: CGCTCATTGCCGATAGTG

Cell Isolation and Co-Culture – Postnatal day one (P1) GFAP.HMOX1 transfected mouse pups were used to generate primary astroglial-neuronal co-cultures. 20 min prior to dissection, mouse pups were separated from the mother. Mice were decapitated and astroglia or neurons were isolated by mechanoenzymatic dissociation of cerebral tissue as previously described (Chopra et al., 1995; Vaya et al., 2007; Jones et al., 2012). Cells were grown in Kaighn's Modification of Ham's F-12 medium and high

glucose DMEM (50:50 v/v) supplemented with 5% heat-inactivated horse serum, 5% heat-inactivated fetal bovine serum and penicillin-streptomycin (50 U/ml and 50 mg/ml, respectively). Cells were seeded in either T-75 mm or T-25 mm^2 flasks, 6 well plates or Transwell Permeable Supports 24 mm Inserts (VWR) at a density of 1.0 x 10^5-1.2 x 10^6 cells/mL and incubated at 37°C in humidified 95% air-5% CO_2. Astroglia cultures were incubated initially for 6 h, after which they were vigorously shaken 18-20 times followed by replacement with fresh medium to remove adherent oligodendroglia and microglia from the astrocytic monolayers. The cultures were maintained under the above-mentioned conditions for 5-16 days at which time more than 98% of the cells comprising the monolayer were astroglial or neuronal as determined by immunohistochemical labeling for the astrocyte-specific marker, GFAP or neurofilament (NF), respectively (Chopra et al., 1995). Neurons were seeded on the bottom of 6-well plates, below the astroglial feeder layer seeded on the Transwell Permeable Inserts. Cytosine β-D-arabinofuranoside (Ara-C) (Sigma) was added to a final concentration of 3 μM in order to prevent glial overgrowth among neurons. This addition was only made once, meaning Ara-C concentration was diluted by 25-50% by the time of harvest.

Western Blot Analysis – Primary cells were lysed with ice-cold RIPA buffer (150 mM NaCl, 1% NP-40, 0.5% sodium deoxycholate, 50 mM Tris-HCl pH 8.0, 40 mM NaF, and protease inhibitors) and incubated on ice for 10 min. Adherent cells were detached using a rubber scraper and collected, followed by an incubation period of 30 min at 4°C with constant agitation. The cell suspension was centrifuged at 13000 rpm for 20 min at 4°C and the subsequent supernatant was stored at -80°C until further use. The DC Protein Assay kit (Bio-Rad) was used to measure protein concentrations prior to

Western blot analysis. Protein samples were boiled for 5 min in the presence of 4X SDS Loading Dye (0.2 M Tris-HCl pH 6.8, 0.2% SDS, 40% glycerol, 0.05 M EDTA pH 8.0, 0.04 µg/mL beta-mercaptoethanol) before electrophoresis on 10% SDS-PAGE and transferred to a polyvinylidene fluoride (PVDF) membrane with 0.2 µm pore size (Bio-Rad). Anti-protein mouse, rat or rabbit monoclonal antibody (mAb) or polyclonal antibody (pAb) (TH, Millipore Bioscience Research Reagents, Clone No. 152; DAT, Abcam, Clone No. 468; alpha-synuclein, BD Biosciences, Clone No. 46; Caspase-3, R&D Systems, Clone No. 269518; LC3B, Cell Signaling, Clone No. 2775) at 1:1000 and anti-mouse, anti-rat or anti-rabbit IgG HRP (Jackson ImmunoResearch) at 1:2000 were used to blot membranes. As an internal control, anti-actin (MediMabs, Clone No. C4) at 1:2000 and anti-mouse IgG HRP (Jackson ImmunoResearch) at 1:2000 were used to re-blot mildly stripped membranes. Amersham ECL Western Blotting Detection Reagent was used for development and protein expression visualization (GE Healthcare Life Sciences).

Immunofluorescence – Coronal brain sections (40 µm) were cut on a Lancer vibratome (1000 Series; Lancer). Sections were incubated with either anti-TH mAb (Thermo Fisher, Clone No. 185) or anti-HO-1 pAb (Enzo Life Sciences, Clone No. 896), followed by donkey anti-rabbit or donkey anti-mouse Cy3-labeled IgG (Jackson ImmunoResearch). After washing, the slides were incubated with either anti-alpha-synuclein mAb (BD Biosciences, Clone No. 46) or anti-MnSOD pAb (BD Biosciences, Clone No. 19), respectively, followed by goat anti-mouse FITC-labeled IgG (Jackson ImmunoResearch). The sections were analyzed using a Carl Zeiss LSM 5 Pascal laser-scanning confocal imaging microscope.

Fluorescence-Activated Cell Sorting (FACS) – Primary cell cultures were washed twice with D-PBS, trypsonized for at least 5 min and washed once more with D-PBS. All medium, washes and cell suspension were collected in a sterile 50 mL tube, followed by centrifugation at 500 x g for 10 min at 21°C. The supernatant was discarded and the pellet was subsequently washed with D-PBS, followed by another centrifugation at 500 x g for 10 min at 21°C. The cell pellet was resuspended in 1X binding buffer. The Annexin V Apoptosis Detection Kit (eBioscience) was used according to manufacturer's instructions. Cells exposed to Staurosporine (0.125-0.5 μM; Sigma), an apoptotic inducer, 18-24 h prior to sample collection served as positive controls for apoptosis. The BD LSR Fortessa Analyzer (BD Biosciences) was used in combination with BD FACSDiva and FlowJo computer software programs for all FACS experiments.

Statistics – All data are expressed as means ± SEM. Statistical significance between control and experimental values was determined using Student's t test (paired, 2-tailed, 95% confidence interval). Statistical significance was set at $p < 0.05$.

RESULTS

Using RT-qPCR to measure relative mRNA expression levels in SN and STM from 19-month old GFAP.HMOX1 mice compared to age-matched WT controls, a broad genetic screen was conducted using a number of different genes from pathways known to be implicated in the pathogenesis of PD. The screen interrogated the DA system, protein aggregation, oxidative stress, apoptosis, autophagy and mitophagy, mitochondrial biogenesis and reelin expression. In addition to *in vivo* samples, relative mRNA expression levels were also assessed *in vitro* in primary astrocyte/neuron co-cultures from GFAP.HMOX1 mice using RT-qPCR. All co-cultures used for mRNA analysis were grown for 7 days under optimized conditions. Select genes from each pathway were analyzed at the protein expression level using a variety of techniques, including Western blot, immunofluorescence and FACS.

MiRNAs negatively regulate mRNA expression via targeted mRNA cleavage, mRNA degradation or protein translation repression. Our group recently employed microchip assays, in combination with RT-qPCR for validation, to elucidate miRNA expression profile alterations in *HMOX1*- and sham-transfected rat astroglia (Lin et al., 2015). The altered miRNAs identified in the latter study were amongst the miRNA screened in the present investigation. Expression levels of miRNAs with putative targets in each of the above mentioned pathways were also analyzed using RT-qPCR.

MiRNA Screen

A broad miRNA screen was conducted, looking specifically at miRNA previously identified as showing altered expression profiles in *HMOX1* overexpression systems (Lin et al., 2015) or as having a putative gene target in one or more of the above-

mentioned pathways. *In vivo* and *in vitro* results are shown in Table 3 and Table 4, respectively. In *HMOX1*-transfected rat astrocytes, rno-miR-140*, rno-miR-17 and rno-miR-16 were significantly upregulated (Lin et al., 2015). Similarly, these miRNA were significantly upregulated in GFAP.HMOX1 SN and STM as well as primary TG astrocytes and TG neurons co-cultures compared to control preparations ($p < 0.05 – 0.001$) (Table 4; Table 5). Furthermore, rno-miR-206, rno-miR-181a, rno-miR-138 and rno-miR-29c were significantly downregulated in *HMOX1*-transfected rat astrocytes compared to sham-transfected rat astrocytes (Lin et al., 2015). While mmu-miR-181a was significantly downregulated in TG STM compared to WT STM ($p < 0.001$) and mmu-miR-206 was significantly downregulated in primary TG astrocytes co-cultured with primary TG neurons compared to WT preparations ($p < 0.05$), the remainder of these miRNA expression levels were either not significantly altered or significantly upregulated in TG samples compared to WT controls ($p < 0.05 – 0.001$) (Table 4; Table 5). Key miRNA from this broad genetic screen will be discussed further below in relation to their putative mRNA target(s).

Table 3. *In vivo* miRNA results. Total RNA was purified from SN and STM of 19-month old TG GFAP.HMOX1 brains and compared to age-matched WT controls, followed by cDNA synthesis and amplification. The Applied Biosystems 7500 Fast RT-qPCR System was used to quantify miRNA with SensiFast SYBR Lo-ROX kit according to manufacturer's instructions. Calculation of respective fold changes by ΔΔCt method in TG GFAP.HMOX1 mice relative to WT control preparations. N = 5 per group. *p < 0.05; **p < 0.01; ***p < 0.001. Data is presented ± SEM.

MicroRNA	Substantia Nigra		Striatum	
Name	**Fold Change**	**P-value**	**Fold Change**	**P-value**
mmu-miR-7a	1.483 ± 0.266	N.S.	1.230 ± 0.251	N.S.
mmu-miR-7b	0.973 ± 0.145	N.S.	1.295 ± 0.249	N.S.
mmu-miR-153	0.696 ± 0.139	*	0.674 ± 0.133	*
mmu-miR-223	0.805 ± 0.086	*	0.710 ± 0.17	***
mmu-miR-133b	1.300 ± 0.171	N.S.	4.094 ± 0.793	***
mmu-miR-145	1.083 ± 0.134	N.S.	1.233 ± 0.112	*
mmu-miR-325	0.681 ± 0.102	**	0.613 ± 0.187	*
mmu-miR-34a-5p	2.312 ± 0.577	*	1.749 ± 0.316	*
mmu-miR-208b	0.694 ± 0.15	N.S.	0.455 ± 0.076	***
mmu-miR-208a-3p	0.386 ± 0.085	***	0.504 ± 0.136	**
mmu-miR-138	1.831 ± 0.377	*	1.079 ± 0.244	N.S.
mmu-miR-181a	1.227 ± 0.32	N.S.	0.674 ± 0.071	***
mmu-miR-29c	3.545 ± 0.577	***	2.259 ± 0.409	**
mmu-miR-206	1.431 ± 0.297	N.S.	1.120 ± 0.224	N.S.
mmu-miR-16	5.107 ± 1.065	***	2.014 ± 0.441	*
mmu-miR-17	6.365 ± 1.693	**	2.196 ± 0.412	**
mmu-miR-140*	2.600 ± 0.568	***	3.910 ± 0.646	***
mmu-miR-137-5p	1.616 ± 0.467	N.S.	2.447 ± 0.577	*
mmu-miR-137-3p	2.075 ± 0.577	N.S.	1.597 ± 0.445	N.S.
mmu-miR-200c-3p	0.93 ± 0.189	N.S.	0.506 ± 0.123	***
mmu-miR-128-5p	0.243 ± 0.058	***	1.069 ± 0.152	N.S.
mmu-miR-128-3p	1.642 ± 0.393	N.S.	2.322 ± 0.449	**

N.S. – not significant

Table 4. *In vitro* miRNA results. Total RNA was purified from astrocytes and neurons of TG GFAP.HMOX1 brains and compared to age-matched WT controls, followed by cDNA synthesis and amplification. The Applied Biosystems 7500 Fast RT-qPCR System was used to quantify miRNA with SensiFast SYBR Lo-ROX kit according to manufacturer's instructions. Calculation of respective fold changes by ΔΔCt method in TG GFAP.HMOX1 mice relative to WT control preparations. N = 5 per group. *p < 0.05; **p < 0.01; ***p < 0.001. Data is SEM. All co-cultures were maintained for 7 days, unless otherwise indicated.

MicroRNA Name	Astrocytes		Neurons	
	Fold Change	P-value	Fold Change	P-value
mmu-miR-7a (3-day cultures)	0.918 ± 0.323	N.S.	3.519 ± 0.863	*
mmu-miR-7b (3-day cultures)	0.488 ± 0.165	**	3.516 ± 0.758	**
mmu-miR-153 (3-day cultures)	0.288 ± 0.054	***	0.551 ± 0.16	*
mmu-miR-223 (3-day cultures)	0.268 ± 0.084	***	0.295 ± 0.02	***
mmu-miR-7a	0.627 ± 0.093	**	1.776 ± 0.494	N.S.
mmu-miR-7b	1.266 ± 0.239	N.S.	1.772 ± 0.616	N.S.
mmu-miR-153	4.986 ± 1.205	**	2.984 ± 0.766	N.S.
mmu-miR-223	1.603 ± 0.474	N.S.	3.804 ± 1.654	N.S.
mmu-miR-133b	7.284 ± 1.951	**	5.830 ± 1.505	*
mmu-miR-145	2.355 ± 0.567	*	1.889 ± 0.038	*
mmu-miR-325	0.632 ± 0.103	*	7.140 ± 3.167	N.S.
mmu-miR-34a-5p	16.265 ± 6.168	*	4.170 ± 1.196	*
mmu-miR-208b	1.354 ± 0.538	N.S.	11.345 ± 5.811	N.S.
mmu-miR-208a-3p	0.496 ± 0.08	*	2.833 ± 1.129	N.S.
mmu-miR-138	1.219 ± 0.182	N.S.	4.337 ± 0.711	**
mmu-miR-181a	2.247 ± 0.468	*	1.428 ± 0.102	**
mmu-miR-29c	2.080 ± 0.485	N.S.	13.954 ± 3.583	**
mmu-miR-206	0.546 ± 0.147	*	10.241 ± 2.99	*
mmu-miR-16	10.913 ± 3.887	*	1.798 ± 0.198	**
mmu-miR-17	4.857 ± 1.308	*	5.573 ± 1.154	**
mmu-miR-140*	5.773 ± 1.73	*	3.721 ± 0.964	*
mmu-miR-137-5p	1.261 ± 0.173	N.S.	12.876 ± 3.816	**
mmu-miR-137-3p	1.309 ± 0.268	N.S.	8.300 ± 0.44	***
mmu-miR-200c-3p	0.425 ± 0.051	**	4.035 ± 1.49	N.S.
mmu-miR-128-5p	1.594 ± 0.232	*	1.185 ± 0.165	N.S.
mmu-miR-128-3p	1.118 ± 0.22	N.S.	4.487 ± 0.606	***

N.S. – not significant

The Dopaminergic System

Genes involved in DA metabolism, TH and DAT, as well genes involved in DA neuron maintenance and support, Nurr1, Pitx3 and LMX1B, were significantly downregulated in TG STM compared to WT controls ($p < 0.05 – 0.001$), while no significant changes were noted in SN (Figure 3A). *In vitro*, TH, DAT, Pixt3 and LMX1B mRNAs were also significantly downregulated in primary neurons co-cultured with primary TG astrocytes for 7 days compared to control preparations employing WT astrocytes ($p < 0.01 – 0.001$), while Nurr1 mRNA remained unchanged (Figure 3B). In primary TG astrocytes co-cultured with primary neurons for 7 days, on the other hand, TH, Nurr1, Pitx3 and LMX1B mRNAs were significantly upregulated compared to WT controls ($p < 0.05 – 0.01$), while DAT mRNA remained unchanged (Figure 3B). Finally, TH and DAT protein expression levels were analyzed further using Western blot. Both TH and DAT proteins were significantly decreased in primary neurons co-cultured with primary astrocytes for 7 days compared to neurons co-cultured with WT astroglia (Figure 3C, D). Furthermore, TH and DAT protein concentrations remained unchanged in primary neurons grown alone, in the absence of contact with primary TG astrocytes (Figure 3C, D).

Putative targets for miR-133b include Pitx3 and DAT, while Nurr1 is a putative target for miR-145 (TargetScan). Mmu-miR-133b and mmu-miR-145 remained unchanged in TG SN compared to WT SN, whereas both miRNAs were significantly upregulated in TG STM compared to WT STM ($p < 0.05 – 0.01$) (Figure 3E). The latter changes correlated inversely with decreased expression of Pitx3, DAT and Nurr1 in TG STM compared to WT STM. In complementary experiments, mmu-miR-133b and mmu-

miR-145 were significantly upregulated in both 7-day neuron and TG astrocyte primary co-cultures compared to WT controls ($p < 0.05 – 0.001$) (Figure 3F), also correlating inversely with decreased DA system gene expression observed *in vitro*.

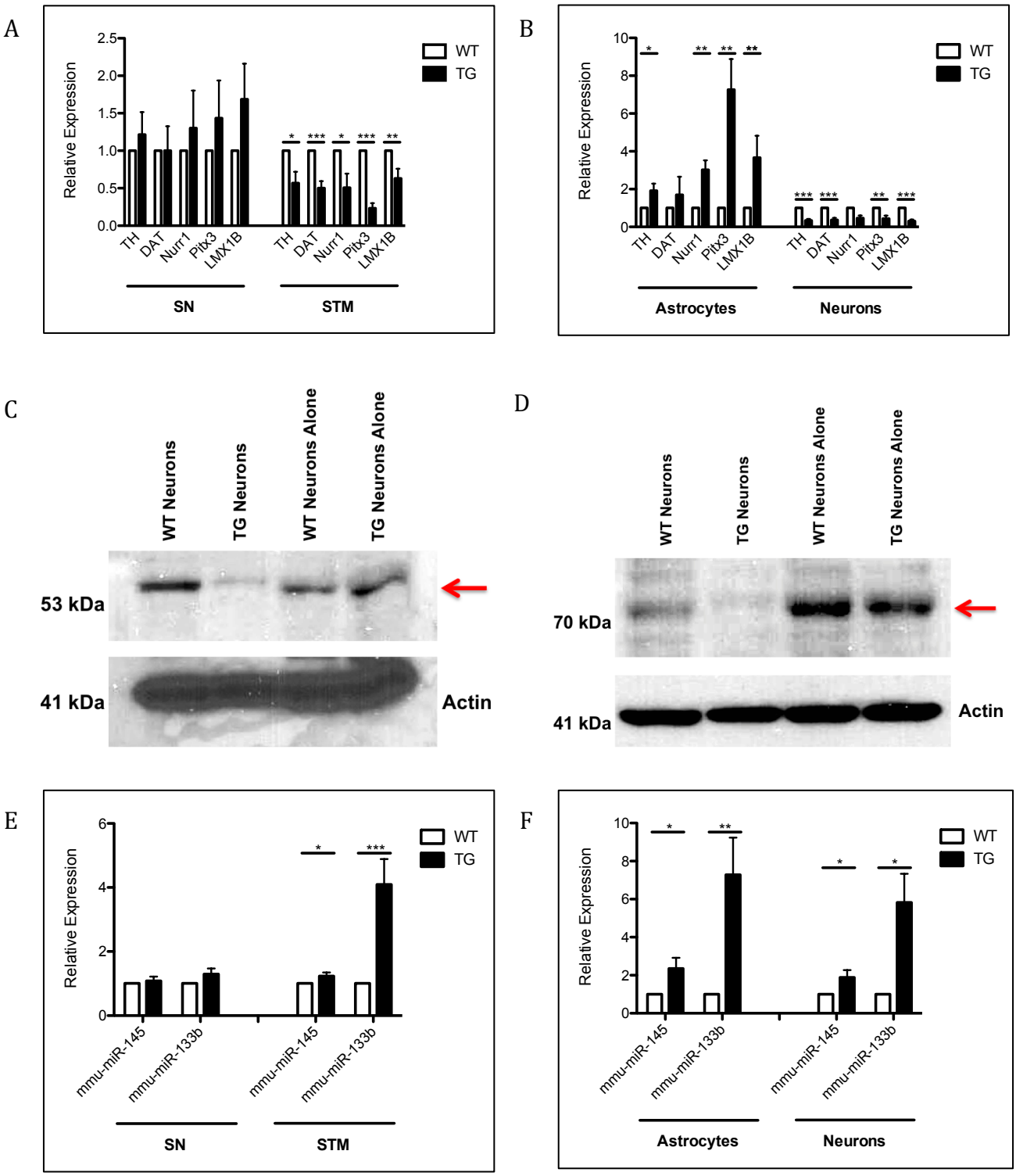

Figure 3. mRNA, protein and miRNA expression levels for the dopaminergic system. *In vivo* samples include SN and STM brain dissections from 19-month old GFAP.HMOX1 mice and are compared to age-matched WT controls. *In vitro* samples include astrocytes and neurons isolated from GFAP.HMOX1 mice and are compared to WT control preparations. For RT-qPCRs, total RNA was purified from samples, followed by cDNA synthesis and amplification. The Applied Biosystems 7500 Fast RT-qPCR System was used to quantify mRNA and miRNA with SensiFast SYBR Lo-ROX kit according to manufacturer's instructions. Calculation of respective fold changes by ΔΔCt method using RT-qPCR in TG GFAP.HMOX1 mice *in vivo* or *in vitro* relative to WT control preparations. For Western blots, whole-cell lysates were collected from *in vitro* samples. Expected molecular weight of TH is 60 kDa (C). Expected molecular weight of DAT is 69 kDa (D). N = 5 per group. *p < 0.05; **p < 0.01; ***p < 0.001. Error bars indicate SEM.

Protein Aggregation

Both alpha-synuclein and ubiquitin mRNA, known to accumulate and play a role in Lewy body formation in PD subjects, were significantly upregulated in TG STM and SN compared to WT controls ($p < 0.05 – 0.001$) (Figure 4A). In relation to alpha-synuclein aggregation, additional negative regulators of alpha-synuclein acting either upstream, CtsB and CtsD, or downstream, Notch1, were measured. CtsB and CtsD mRNAs were significantly downregulated in the STM of TG mice compared to WT controls ($p<0.01 – 0.001$), while CtsD and Notch1 mRNAs were significantly downregulated in the SN of TG mice compared to WT controls ($p < 0.05 – 0.01$) (Figure 4B). Expression levels of Notch1 mRNA in the STM and CtsB mRNA in the SN were not significantly different from WT controls (Figure 4B). Similarly, alpha-synuclein mRNA was significantly upregulated in primary neurons co-cultured with primary TG astrocytes for 7 days compared to WT controls ($p < 0.05$), while ubiquitin mRNA was significantly downregulated ($p < 0.001$) (Figure 4C). In primary TG astrocytes co-cultured with primary neurons for 7 days, both alpha-synuclein and ubiquitin mRNA were significantly upregulated compared to WT controls ($p < 0.001$) (Figure 4C), recapitulating results observed *in vivo*. Alpha-synuclein protein expression level was analyzed further using immunofluorescence and Western blot. Immunofluorescence analysis showed increased alpha-synuclein labeling in the SN of 19-month old male TG mice compared to the SN of age-matched male WT mice (Figure 5). While Western blot analysis *in vitro* showed decreased expression of alpha-synuclein protein in primary neurons co-cultured with primary TG astrocytes for 7 days (data not shown), alpha-synuclein expression was significantly increased in primary neurons co-cultured with primary TG astrocytes for 14

days (Figure 6), possibly underscoring the dual nature (antioxidant or pro-oxidant) of HO-1 in redox homeostasis.

Alpha-synuclein is a putative target of miR-7a, miR-7b, miR-153 and miR-223 (TargetScan). Both mmu-miR-7a and mmu-miR-7b were not significantly changed in TG STM and SN compared to WT controls, however mmu-miR-153 and mmu-miR-223 were significantly downregulated in TG STM and SN compared to WT controls ($p < 0.05 – 0.001$) (Figure 4D). *In vitro*, on the other hand, no significant changes were observed for any of the miRNAs in primary neurons co-cultured with primary TG astrocytes for 7 days (Figure 4F). Similarly, no significant changes were observed for mmu-miR-7b and mmu-miR-223 in primary TG astrocytes co-cultured with primary neurons for 7 days (Figure 4F). However, mmu-miR-7a was significantly downregulated ($p < 0.01$) and mmu-miR-153 was significantly upregulated ($p < 0.01$) in these TG co-cultured astrocytes compared to WT controls (Figure 4F). MiRNA expression levels were then assessed in 3-day primary co-cultures. Interestingly, mmu-miR-153 and mmu-miR-223 were significantly upregulated in both 3-day neuron and TG astrocyte primary co-cultures ($p < 0.05 – 0.001$) (Figure 4E), recapitulating results observed *in vivo*. On the other hand, mmu-miR-7a and mmu-miR-7b remained unchanged in both 3-day neuron and TG astrocyte primary co-cultures compared to WT controls (Figure 4E).

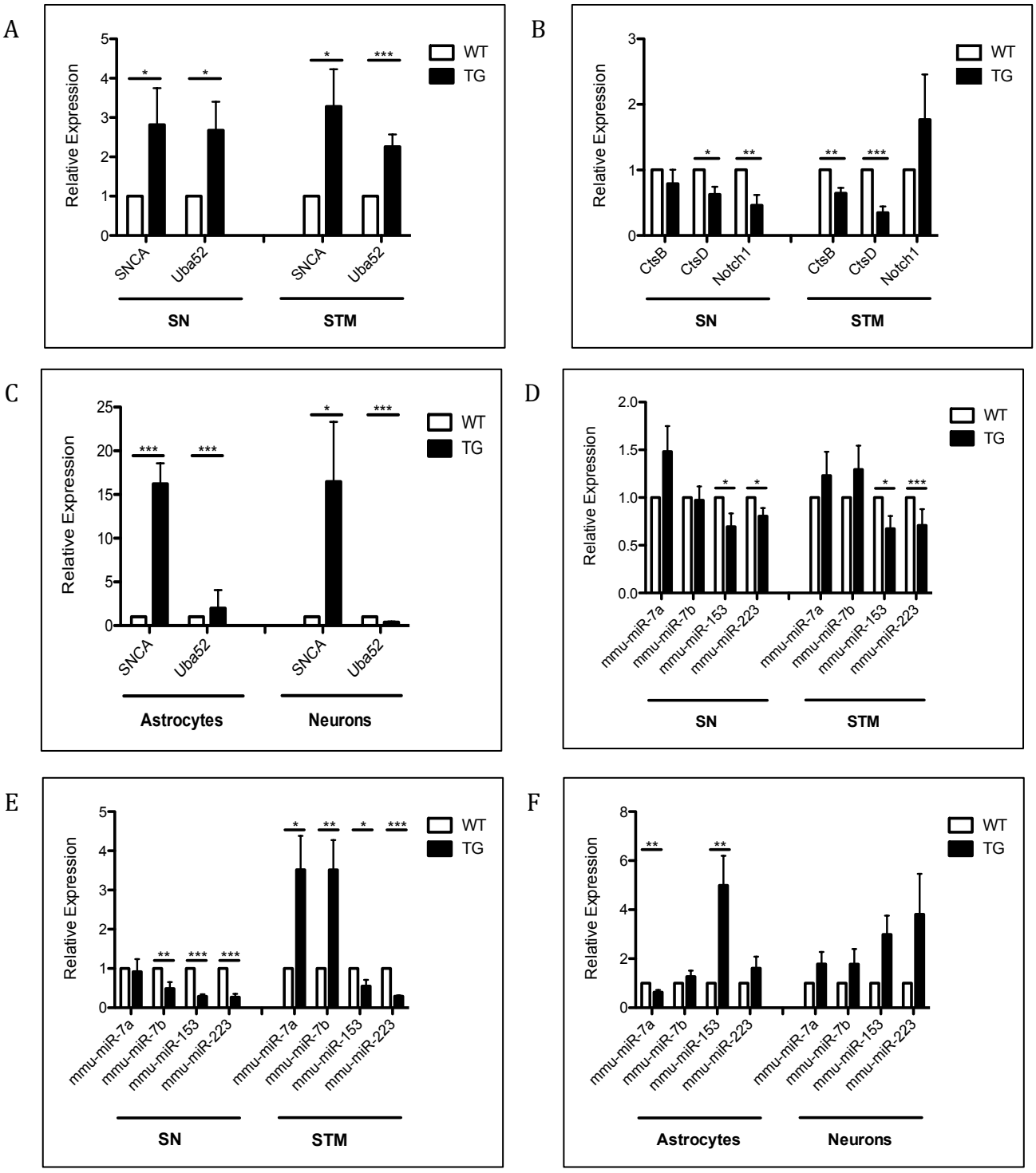

Figure 4. mRNA and miRNA expression levels for protein aggregation in PD. *In vivo* samples include SN and STM brain dissections from 19-month old GFAP.HMOX1 mice and are compared to age-matched WT controls. *In vitro* samples include astrocytes and neurons isolated from GFAP.HMOX1 mice and are compared to WT control preparations. For RT-qPCRs, total RNA was purified from samples, followed by cDNA synthesis and amplification. The Applied Biosystems 7500 Fast RT-qPCR System was used to quantify mRNA and miRNA with SensiFast SYBR Lo-ROX kit according to manufacturer's instructions. Calculation of respective fold changes by ΔΔCt method using RT-qPCR in TG GFAP.HMOX1 mice *in vivo* or *in vitro* relative to WT control preparations. N = 5 per group. *p < 0.05; **p < 0.01; ***p < 0.001. Error bars indicate SEM.

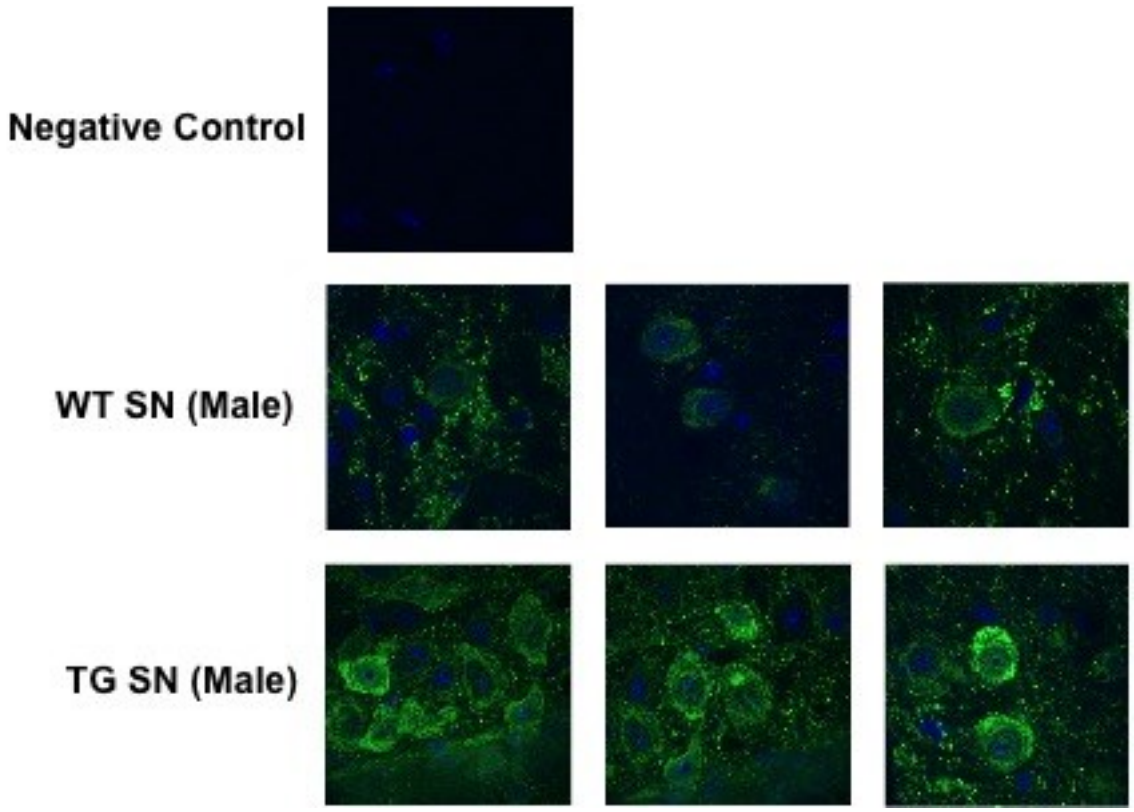

Figure 5. Alpha-synuclein overexpressed in SN of GFAP.HMOX1$^{8.5\text{-}19m}$ TG male mice compared to WT mice. *In vivo* samples include SN brain dissections from 19-month old GFAP.HMOX1 mice and are compared to age-matched WT controls. Coronal brain sections (40 µm) were cut on a Lancer vibratome. The sections were analyzed using a Carl Zeiss LSM 5 Pascal laser-scanning confocal imaging microscope. Alpha-synuclein labeled in green; DAPI (nuclei) labeled in blue. Scale bar, 10 µM. N = 4 per group.

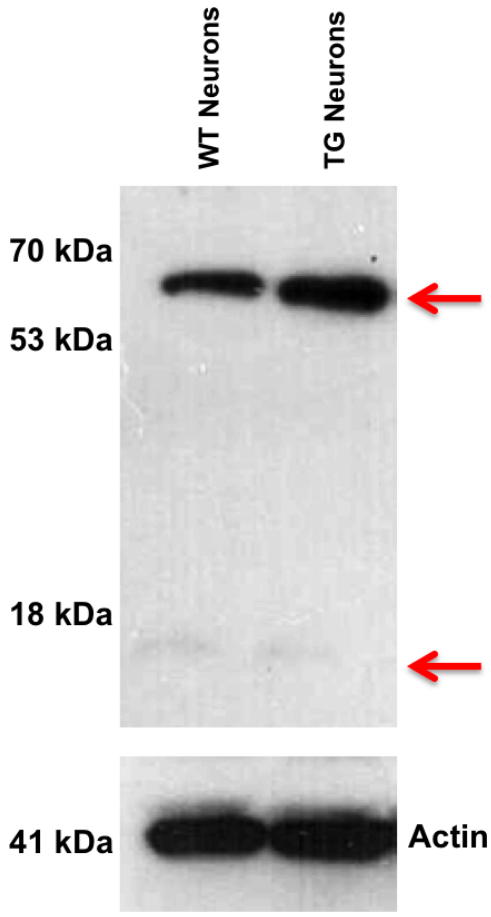

Figure 6. Multimeric alpha-synuclein is overexpressed in primary TG neurons co-cultured with primary GFAP.HMOX1 astrocytes compared to WT preparations. *In vitro* samples include neurons isolated from GFAP.HMOX1 mice and are compared to WT control preparations. Whole-cell lysates were collected from samples. Expected molecular weight of monomeric alpha-synuclein is 14 kDa. N = 4 per group.

Oxidative Stress

Among the genes involved in oxidative stress regulation, both MnSOD and PGC1a mRNAs were significantly upregulated in TG STM and SN compared to WT controls (0.05 – 0.001) (Figure 7A). On the other hand, Sirt1 mRNA was significantly upregulated in SN ($p < 0.01$) and downregulated in STM ($p < 0.001$), while PARP1 mRNA was downregulated in STM ($p < 0.001$), yet unchanged in STM compared to WT controls (Figure 7A). *In vitro*, MnSOD, PGC1a, Sirt1 and PARP1 mRNAs were significantly upregulated in both 7-day neuron and TG astrocyte primary co-cultures ($p < 0.05 – 0.001$), with the exception that PARP1 remained unchanged in primary neurons (Figure 7B). MnSOD protein expression level was analyzed further using immunofluorescence *in vivo*. In SN tissue from GFAP.HMOX1$^{8.5\text{-}19m}$ mice co-labeled with MnSOD (green) and HO-1 (red), neurons displayed increased levels of MnSOD compared to WT SN (Figure 8).

Sirt1 is a putative target of miR-128 (TargetScan). Mmu-miR-128-1-5p was unchanged in TG STM and downregulated in TG SN ($p < 0.001$) compared to WT controls (Figure 7C), correlating inversely with increased Sirt1 mRNA observed in TG SN. However, *in vitro* results did not correlate inversely with Sirt1 mRNA expression levels. Mmu-miR-128-1-5p was significantly upregulated ($p < 0.05$) in primary TG astrocytes co-cultured with primary neurons for 7 days and unchanged in these primary neurons compared to WT controls (Figure 7D).

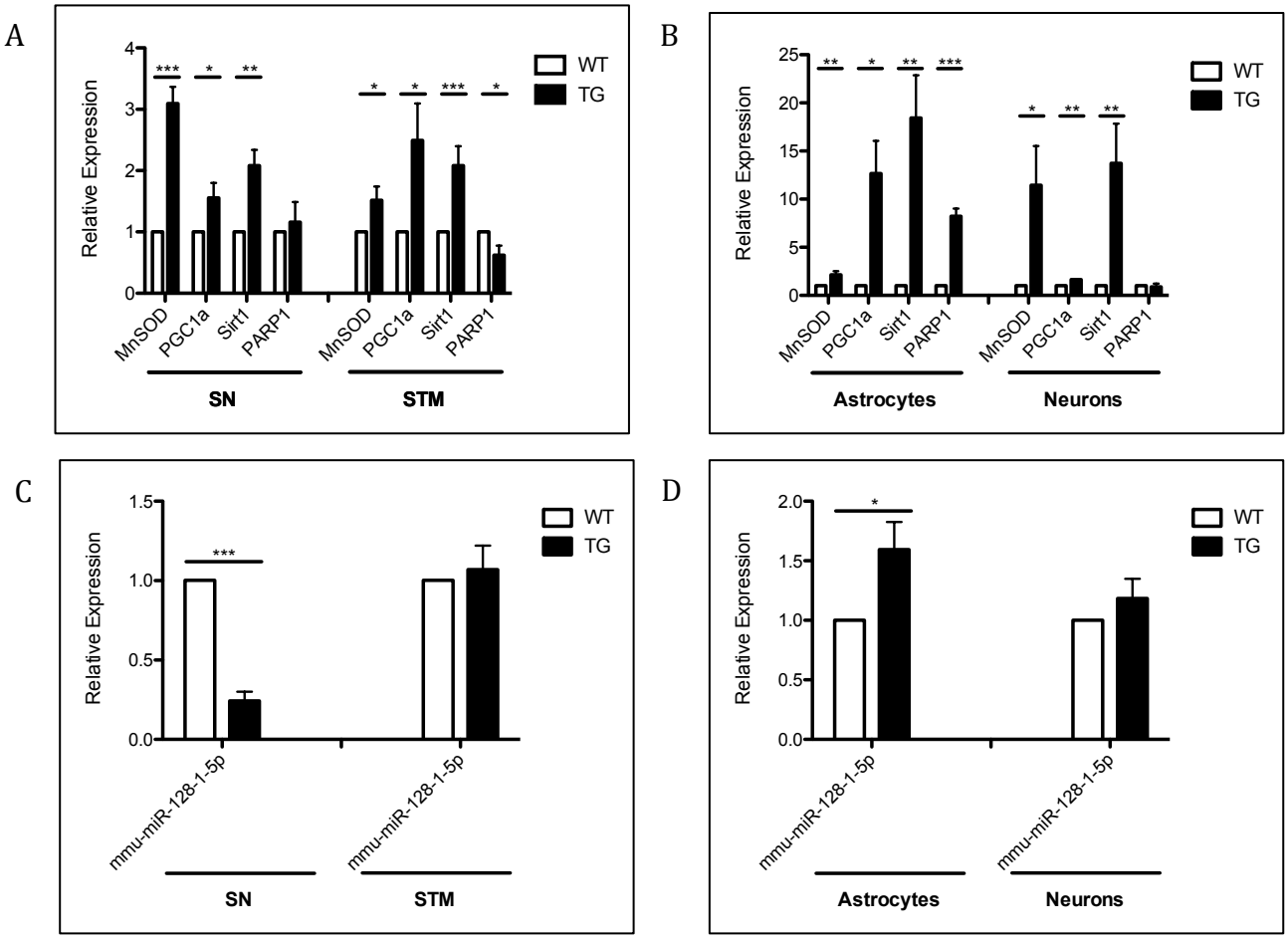

Figure 7. mRNA, protein and miRNA expression levels for markers of oxidative stress. *In vivo* samples include SN and STM brain dissections from 19-month old GFAP.HMOX1 mice and are compared to age-matched WT controls. *In vitro* samples include astrocytes and neurons isolated from GFAP.HMOX1 mice and are compared to WT control preparations. Total RNA was purified from samples, followed by cDNA synthesis and amplification. The Applied Biosystems 7500 Fast RT-qPCR System was used to quantify mRNA and miRNA with SensiFast SYBR Lo-ROX kit according to manufacturer's instructions. Calculation of respective fold changes by ΔΔCt method using RT-qPCR in TG GFAP.HMOX1 mice *in vivo* or *in vitro* relative to WT control preparations. N = 5 per group. *p < 0.05; **p < 0.01; ***p < 0.001. Error bars indicate SEM.

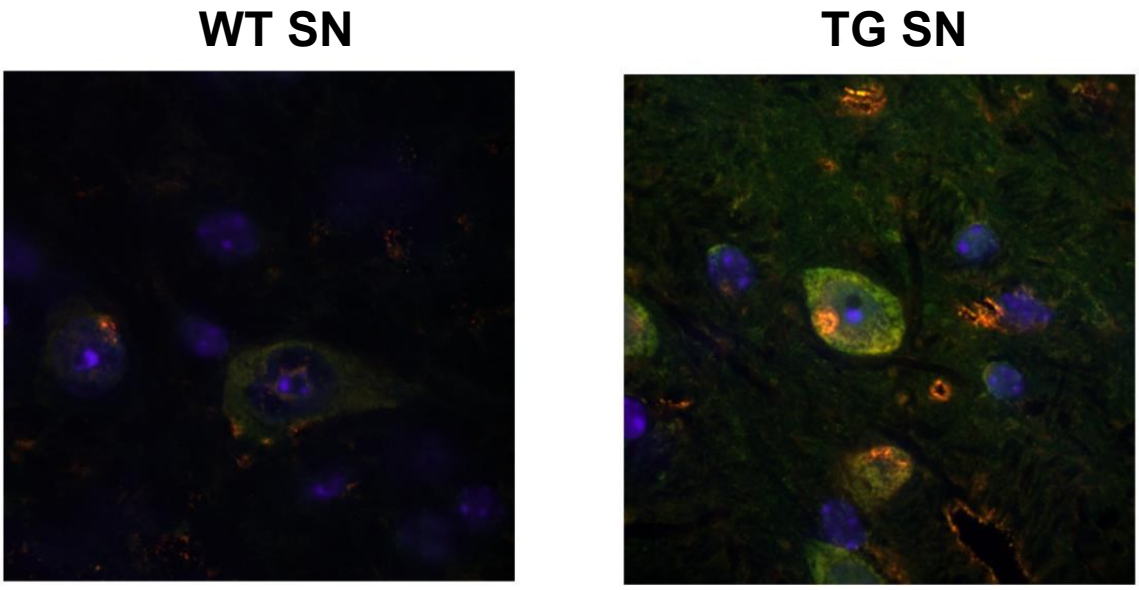

Figure 8. MnSOD is overexpressed in SN of GFAP.HMOX1$^{8.5\text{-}19m}$ TG mice compared to WT mice. *In vivo* samples include SN brain dissections from 19-month old GFAP.HMOX1 mice and are compared to age-matched WT controls. Coronal brain sections (40 μm) were cut on a Lancer vibratome. The sections were analyzed using a Carl Zeiss LSM 5 Pascal laser-scanning confocal imaging microscope. MnSOD labeled in green; HO-1 labeled in red; DAPI labeled in blue. Scale bar, 10 μM. N = 4 per group.

Apoptosis

Several genes involved in the apoptotic pathway were analyzed, including p53, p21, PUMA, Bak, Bax and Bcl2. All apoptotic genes were significantly upregulated at the mRNA level in both TG STM and SN compared to WT controls ($p < 0.05 – 0.001$), with the exception of PUMA in TG STM, which was not significantly different from WT STM controls (Figure 9A). Similar to results observed *in vivo*, p53, p21, PUMA, Bak, Bax and Bcl2 mRNAs were significantly upregulated in both 7-day neuron and TG astrocyte primary co-cultures ($p < 0.05 – 0.001$), with the exception of p53 mRNA in primary neurons co-cultured with primary TG astrocytes for 7 days, which was significantly downregulated ($p < 0.001$) (Figure 9B). Active caspase-3, a crucial mediator of programmed cell death, was analyzed using Western blot. Caspase-3 expression levels were significantly increased in TG neurons co-cultured with TG astrocytes compared to WT preparations (Figure 9C). Apoptotic protein machinery was analyzed further using FACS, which measures early and late stage apoptosis in live cells. In primary TG astrocytes co-cultured with TG neurons for 7 days, early stage apoptosis was significantly increased while late stage apoptosis was significantly decreased (Figure 10A). There was no significant difference in early stage apoptosis between WT and TG primary neurons co-cultured with primary TG astrocytes for 7 days; however these neurons exhibited increased late stage apoptosis compared to WT controls (Figure 10B).

Several miRNAs were selected as potential regulators of genes involved in the apoptotic pathway. MiR-153, miR208a-3p and miR-208b, which putatively target p21 (www.targetscan.org), were all significantly downregulated in TG STM and SN

compared to WT controls ($p < 0.05 – 0.001$) (Figure 9D). This correlates inversely with the increased expression of p21 mRNA observed in TG STM and SN. However, only mmu-miR-208a-3p was similarly downregulated *in vitro* ($p < 0.05$), specifically in primary TG astrocytes co-cultured with primary neurons for 7 days (Figure 9E). All other miRNAs targeting p21 in both 7-day TG astrocyte and neuron primary co-cultures were not significantly altered (Figure 9E). It has previously been shown that apoptosis is regulated by miR-200c-3p (Schickel et al., 2010). Mmu-miR-200c-3p was significantly downregulated in TG STM ($p < 0.001$), yet unchanged in TG SN, compared to WT controls (Figure 9D). Downregulation of miR-200c-3p correlates inversely with apparent upregulation of apoptotic genes observed *in vivo*. In primary TG astrocyte and neuron 7-day co-cultures, mmu-miR-200c-3p was significantly downregulated in astrocytes ($p < 0.01$) and unchanged in neurons compared to WT preparations (Figure 9E). Finally, p53 is a putative target of miR-325 (www.targetscan.org). Mmu-miR-325 was significantly downregulated in TG STM and SN ($p < 0.01 – 0.001$) compared to WT controls (Figure 9D). This correlated inversely with increased expression of p53 mRNA observed in TG STM and SN. In primary TG astrocyte and neuron 7-day co-cultures, mmu-miR-325 was significantly downregulated in astrocytes ($p < 0.05$) and unchanged in neurons compared to WT preparations (Figure 9E).

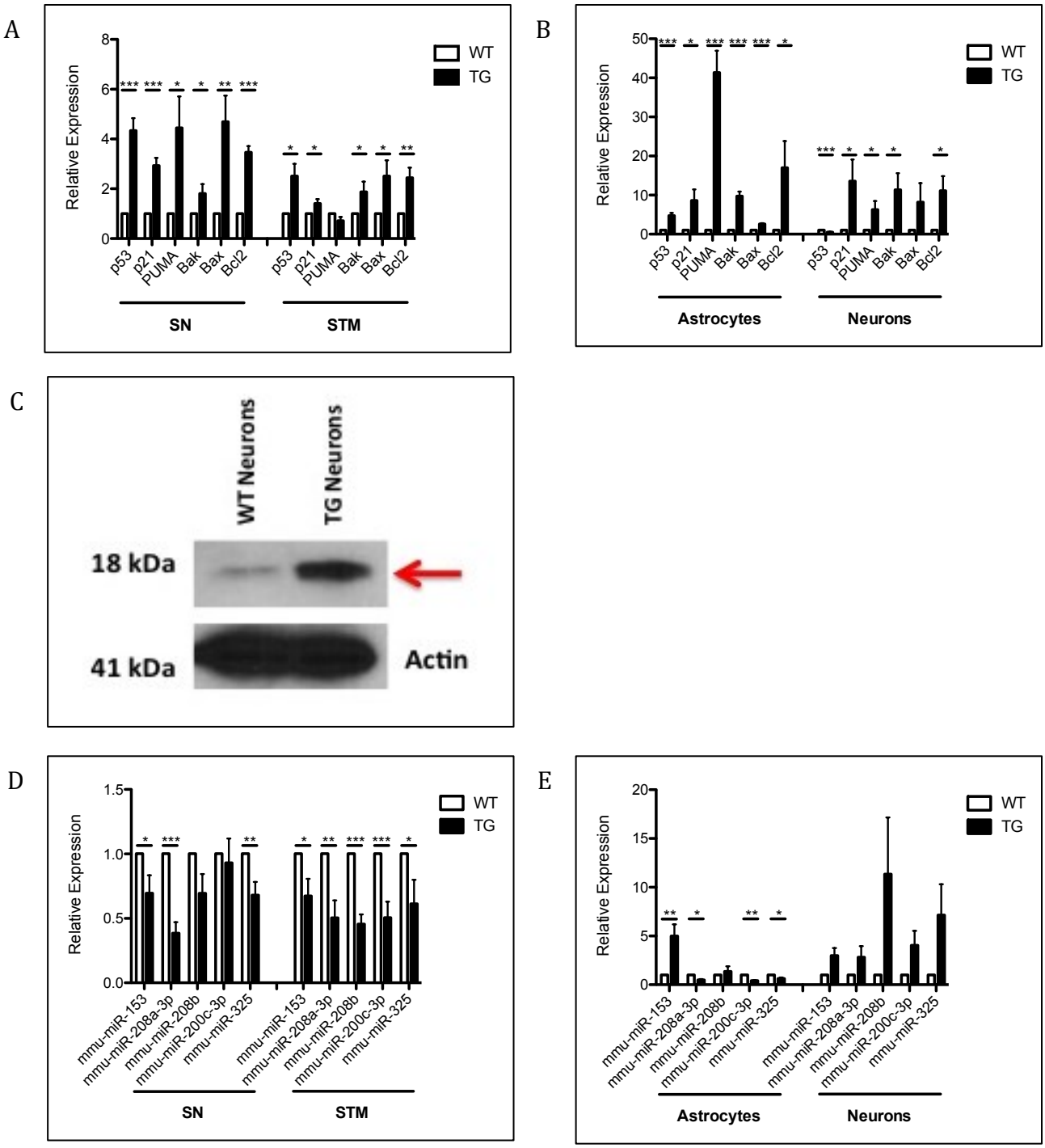

Figure 9. mRNA, protein and miRNA expression levels for apoptotic machinery. *In vivo* samples include SN and STM brain dissections from 19-month old GFAP.HMOX1 mice and are compared to age-matched WT controls. *In vitro* samples include astrocytes and neurons isolated from GFAP.HMOX1 mice and are compared to WT control preparations. For RT-qPCRs, total RNA was purified from samples, followed by cDNA synthesis and amplification. The Applied Biosystems 7500 Fast RT-qPCR System was used to quantify mRNA and miRNA with SensiFast SYBR Lo-ROX kit according to manufacturer's instructions. Calculation of respective fold changes by ΔΔCt method using RT-qPCR in TG GFAP.HMOX1 mice *in vivo* or *in vitro* relative to WT control preparations. For Western blots, whole-cell lysates were collected from *in vitro* samples. Expected molecular weight of cleaved caspase-3 is 17 kDa (C). N = 5 per group. *p < 0.05; **p < 0.01; ***p < 0.001. Error bars indicate SEM.

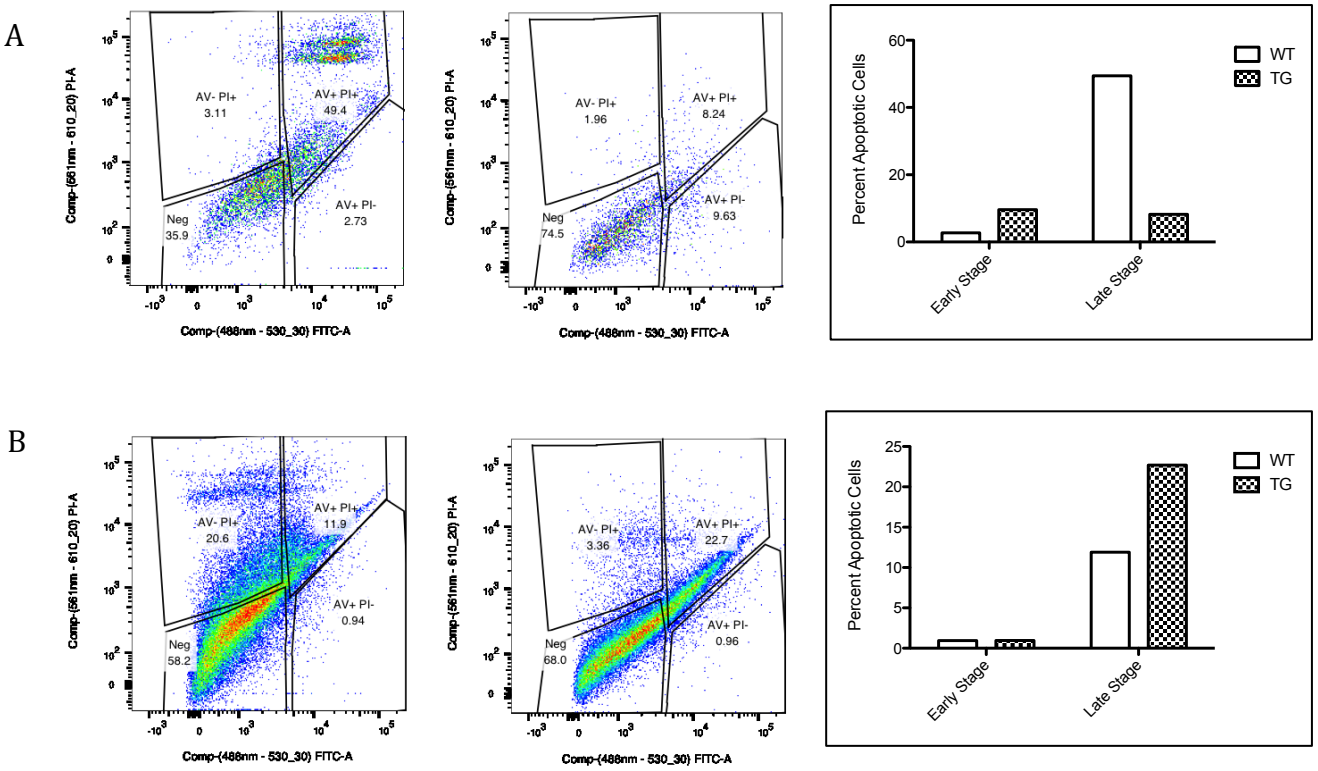

Figure 10. FACS analysis of FITC/PI stained primary GFAP.HMOX1 astrocyte/neuron co-cultures. *In vitro* samples include astrocytes (A) and neurons (B) isolated from GFAP.HMOX1 mice and are compared to WT control preparations. Cells were grown together in co-culture for 14 days. N = 1 per group.

Autophagy and Mitophagy

In terms of the genes involved in autophagy, BECN1, p62 and Hdac6 mRNAs were significantly upregulated in TG STM and SN ($p < 0.05 – 0.001$), while Lamp2 mRNA was significantly upregulated in TG STM ($p < 0.001$) but showed no change in TG SN compared to WT controls (Figure 11A). All autophagic genes, including BECN1, p62, Hdac6 and Lamp2, were significantly upregulated at the mRNA level in both 7-day neuron and TG astrocyte primary co-cultures ($p < 0.05 – 0.001$) compared to WT controls (Figure 11B). The ratio of LC3B-II/LC3B-I, an autophagosome marker in its active membrane-bound and inactive cytosolic forms, respectively, was measured using Western blot. LC3B-II/LC3B-1 was unchanged in primary neurons co-cultured with primary TG astrocytes for 7 days; however this ratio was significantly increased in primary TG astrocytes co-cultured with primary neurons for 7 days compared to WT controls (Figure 11C).

We looked more specifically at genes involved in mitophagy, otherwise known as mitochondrial macroautophagy, including Parkin, PTEN, PINK1 and DJ-1. Parkin, PTEN and PINK1 mRNAs were significantly upregulated in TG SN ($p < 0.05 – 0.001$), yet unchanged in TG STM compared to WT controls (Figure 12A). DJ-1 mRNA was found to be unchanged in TG SN and significantly downregulated in TG STM compared to WT controls ($p < 0.001$) (Figure 12A). Similarly, Parkin, PTEN, PINK1 and DJ-1 mRNAs were significantly upregulated in both 7-day neuron and TG astrocyte primary co-cultures ($p < 0.05 – 0.001$), with the exception of DJ-1 mRNA in primary neurons co-cultured with primary TG astrocytes for 7 days, which was significantly downregulated compared to WT controls ($p < 0.001$) (Figure 12B).

Another putative target of miR-325 is p62 (www.targetscan.org). Mmu-miR-325 was significantly downregulated in TG STM and SN ($p < 0.05 – 0.01$) compared to WT controls, correlating inversely with increased expression of p62 in TG STM and SN (Figure 11D). In primary TG astrocyte and neuron 7-day co-cultures, mmu-miR-325 was significantly downregulated in astrocytes ($p < 0.05$) and unchanged in neurons compared to WT preparations (Figure 11E).

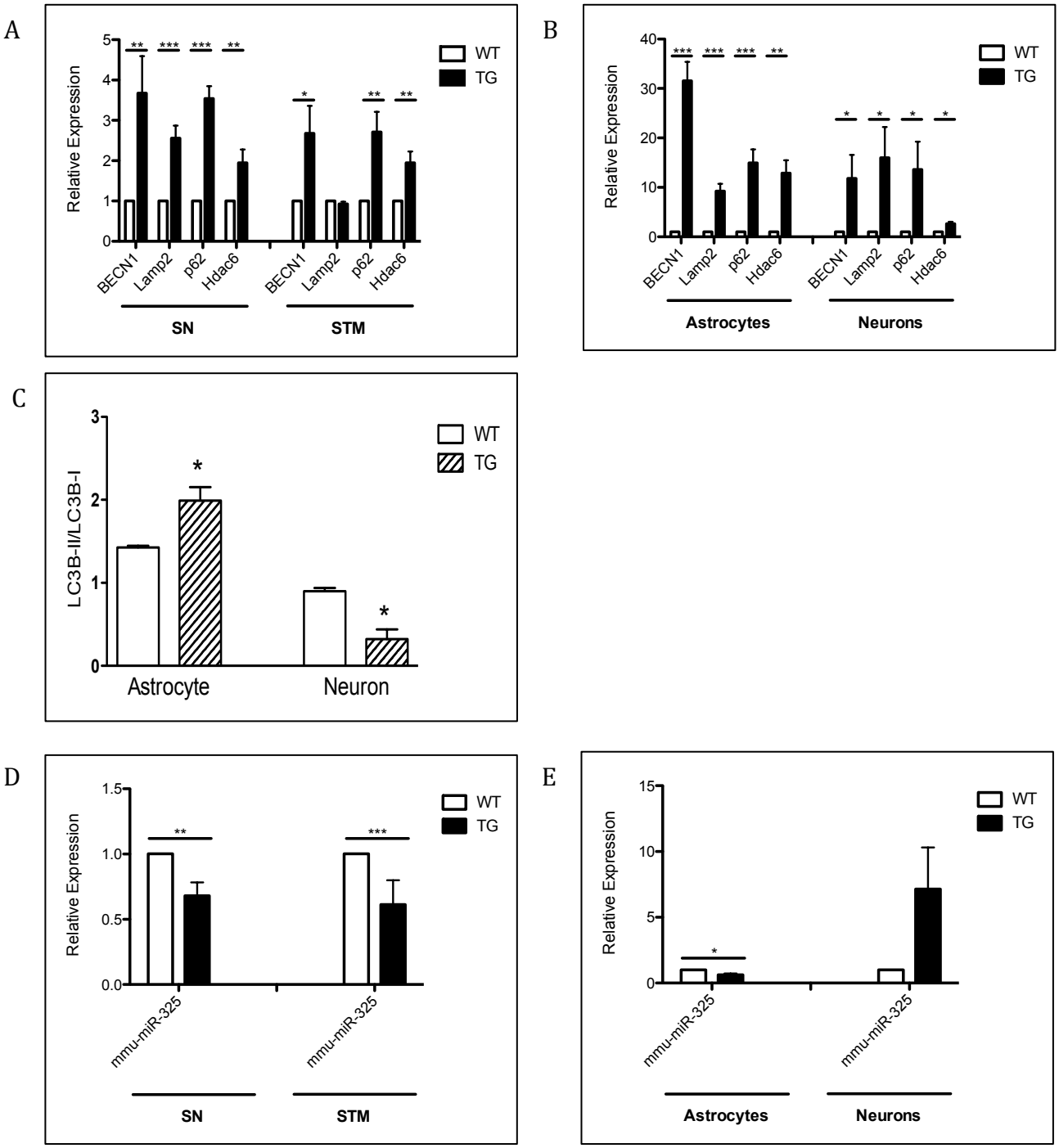

Figure 11. mRNA, protein and miRNA expression levels for autophagic machinery. *In vivo* samples include SN and STM brain dissections from 19-month old GFAP.HMOX1 mice and are compared to age-matched WT controls. *In vitro* samples include astrocytes and neurons isolated from GFAP.HMOX1 mice and are compared to WT control preparations. For RT-qPCRs, total RNA was purified from samples, followed by cDNA synthesis and amplification. The Applied Biosystems 7500 Fast RT-qPCR System was used to quantify mRNA and miRNA with SensiFast SYBR Lo-ROX kit according to manufacturer's instructions. Calculation of respective fold changes by ΔΔCt method using RT-qPCR in TG GFAP.HMOX1 mice *in vivo* or *in vitro* relative to WT control preparations. For Western blots, whole-cell lysates were collected from *in vitro* samples. Expected molecular weight of LC3B-I is 16 kDa and LC3B-II is 14 kDa (C). N = 5 per group. *p < 0.05; **p < 0.01; ***p < 0.001. Error bars indicate SEM.

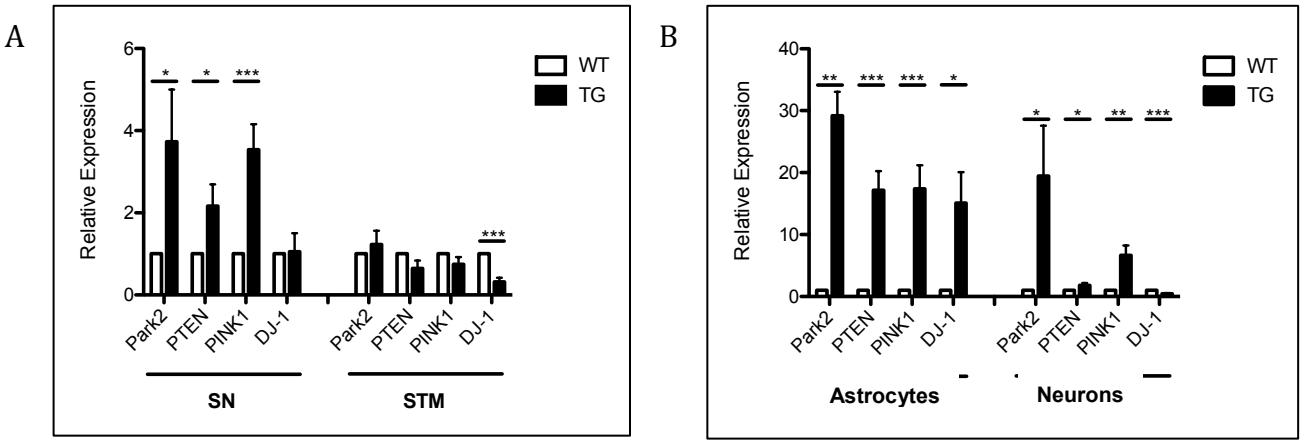

Figure 12. mRNA expression levels for genes involved in mitophagy. *In vivo* samples include SN and STM brain dissections from 19-month old GFAP.HMOX1 mice and are compared to age-matched WT controls. *In vitro* samples include astrocytes and neurons isolated from GFAP.HMOX1 mice and are compared to WT control preparations. Total RNA was purified from samples, followed by cDNA synthesis and amplification. The Applied Biosystems 7500 Fast RT-qPCR System was used to quantify mRNA with SensiFast SYBR Lo-ROX kit according to manufacturer's instructions. Calculation of respective fold changes by ΔΔCt method using RT-qPCR in TG GFAP.HMOX1 mice *in vivo* or *in vitro* relative to WT control preparations. N = 5 per group. *p < 0.05; **p < 0.01; ***p < 0.001. Error bars indicate SEM.

Mitochondrial Biogenesis

Mitochondrial biogenesis, involving Mfn1, Mfn2 and OPA-1 in fusion and Drp1 in fission, is known to be imbalanced in PD (Celardo et al., 2014). Mfn1, Mfn2 and OPA-1 mRNAs were upregulated in TG STM and SN ($p < 0.05 – 0.001$), while Drp1 was significantly downregulated in TG STM and SN ($p < 0.001$) (Figure 13A), supporting an imbalance in mitochondrial biogenesis. Mfn1, Mfn2 and OPA-1 were also significantly upregulated in both 7-day neuron and TG astrocyte primary co-cultures ($p < 0.05 – 0.001$), with the exception of Mfn1 in primary neurons co-cultured with primary TG astrocytes for 7 days, which was not significantly different from WT controls (Figure 13B). Drp1 was significantly upregulated in primary TG astrocytes co-cultured with primary neurons for 7 days ($p < 0.001$) and unchanged in primary neurons co-cultured with primary TG astrocytes for 7 days (Figure 13B).

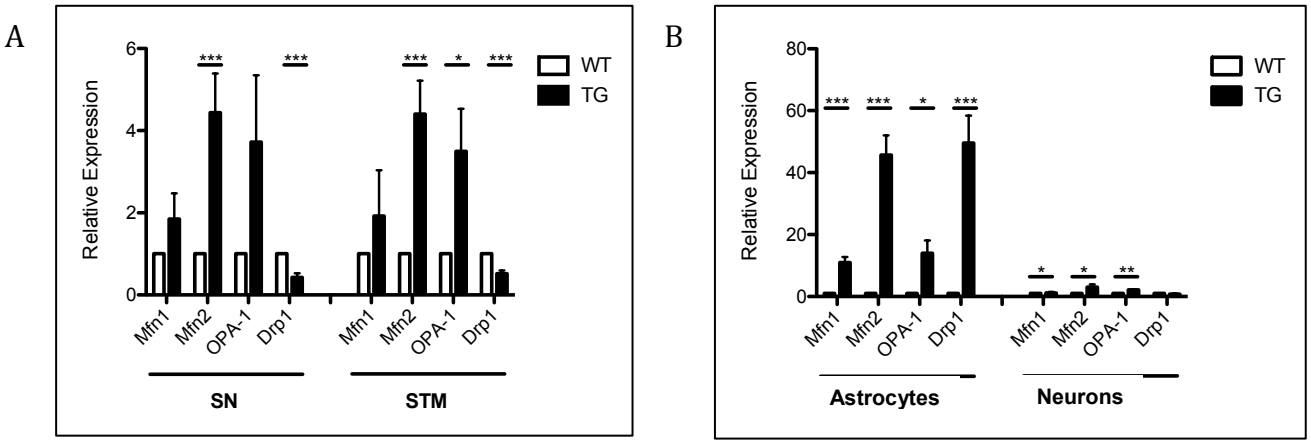

Figure 13. mRNA expression levels for genes involved in mitochondrial biogenesis. *In vivo* samples include SN and STM brain dissections from 19-month old GFAP.HMOX1 mice and are compared to age-matched WT controls. *In vitro* samples include astrocytes and neurons isolated from GFAP.HMOX1 mice and are compared to WT control preparations. Total RNA was purified from samples, followed by cDNA synthesis and amplification. The Applied Biosystems 7500 Fast RT-qPCR System was used to quantify mRNA with SensiFast SYBR Lo-ROX kit according to manufacturer's instructions. Calculation of respective fold changes by ΔΔCt method using RT-qPCR in TG GFAP.HMOX1 mice *in vivo* or *in vitro* relative to WT control preparations. N = 5 per group. *$p < 0.05$; **$p < 0.01$; ***$p < 0.001$. Error bars indicate SEM.

Reelin

Reelin is known to play a role in synaptic plasticity, learning and memory (Botella-Lopez et al., 2006). Decreased reelin is most commonly observed in developmental disorders, such as schizophrenia and bipolar disorder; however recent evidence has implicated increased reelin in neurodegenerative disorders, including PD and AD (Botella-Lopez et al., 2006). Reelin mRNA was significantly upregulated in TG SN ($p < 0.05$) and unchanged in TG STM compared to WT controls (Figure 14A). GAD67 mRNA, which acts downstream of reelin (Guidotti et al., 2000), was significantly upregulated in both TG STM and SN compared to WT controls (Figure 14A). Similarly, reelin and GAD67 mRNAs were significantly upregulated in both 7-day neuron and TG astrocyte primary co-cultures ($p < 0.05 – 0.01$) (Figure 14B).

Reelin is a putative target of miR-200c-3p (Stary et al., 2015). Mmu-miR-200c-3p was significantly downregulated in TG STM ($p < 0.001$), yet unchanged in TG SN, compared to WT controls (Figure 14C). Downregulation of miR-200c-3p correlates inversely with increased expression of reelin mRNA in TG SN. In primary TG astrocyte and neuron 7-day co-cultures, mmu-miR-200c-3p was significantly downregulated in astrocytes ($p < 0.01$) and unchanged in neurons compared to WT preparations (Figure 14D).

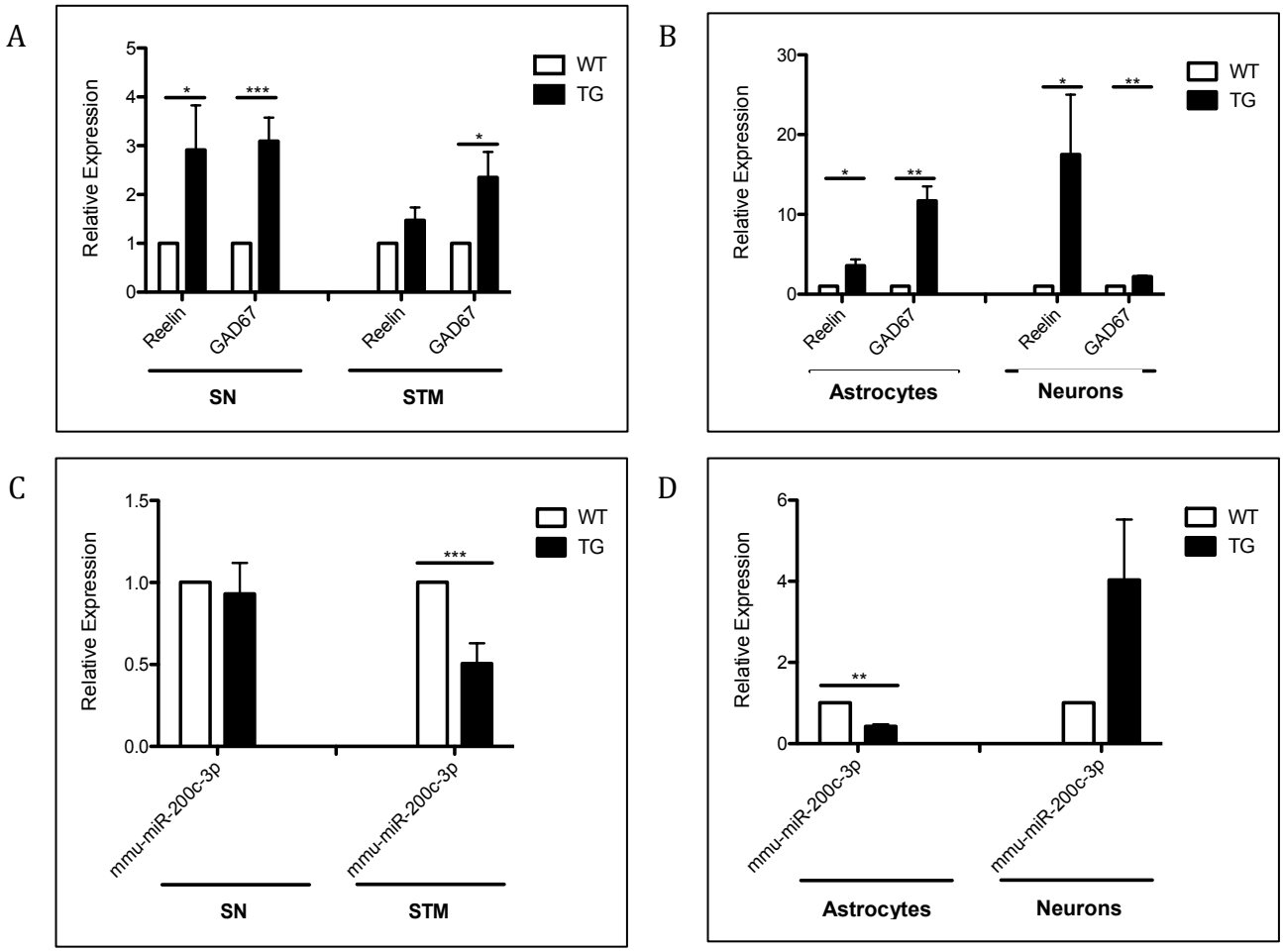

Figure 14. mRNA and miRNA expression levels for genes involved in the reelin pathway. *In vivo* samples include SN and STM brain dissections from 19-month old GFAP.HMOX1 mice and are compared to age-matched WT controls. *In vitro* samples include astrocytes and neurons isolated from GFAP.HMOX1 mice and are compared to WT control preparations. Total RNA was purified from samples, followed by cDNA synthesis and amplification. The Applied Biosystems 7500 Fast RT-qPCR System was used to quantify mRNA and miRNA with SensiFast SYBR Lo-ROX kit according to manufacturer's instructions. Calculation of respective fold changes by ΔΔCt method using RT-qPCR in TG GFAP.HMOX1 mice *in vivo* or *in vitro* relative to WT control preparations. N = 5 per group. *p < 0.05; **p < 0.01; ***p < 0.001. Error bars indicate SEM.

DISCUSSION

The GFAP.HMOX1$^{8.5\text{-}19m}$ TG mouse model of PD exhibits robust neurochemical, pathological and behavioural evidence recapitulating the disease (Song et al., 2013; and unpublished data). The current study was aimed to further characterize the model at the molecular level, targeting pathways that are known to play a role in PD pathogenesis. These pathways include the DA system, protein aggregation and Lewy body formation, oxidative stress, apoptosis, autophagy and mitophagy, mitochondrial biogenesis and reelin activity. A broad array of miRNAs and their mRNA targets involved in each of these pathways were analyzed via RT-qPCR in the GFAP.HMOX1$^{8.5\text{-}19m}$ TG mouse model, followed by protein expression analysis of key proteins from each pathway.

MiRNA Screen

To correlate glial HO-1 overexpression with altered miRNA patterns, which have been linked to core neuropathological features of PD, our group recently employed microchip assays and RT-qPCR to assess miRNA profiles of *HMOX1*- and sham-transfected primary rat astrocytes. These altered miRNAs were also analyzed in the current study, in both *in vivo* and *in vitro* samples from GFAP.HMOX1 TG mice. This broad genetic screen has helped to delineate which miRNAs anti-correlate with mRNA and protein expression levels, validating the pursuit of further mechanistic studies in our model, as discussed below.

In *HMOX1*-transfected astrocytes, rno-miR-140*, rno-miR-17 and rno-miR-16 were found to be significantly upregulated (Lin et al., 2015), a result that was recapitulated in both *in vivo* and *in vitro* preparations from GFAP.HMOX1 mice

compared to WT controls (Table 4; Table 5). Oxidative stress is a potent regulator of large miRNA networks, including miR-140*, miR-17 and miR-16 (Simone et al., 2009; Wagner-Ecker et al., 2010; Howell et al., 2013; Fatima et al., 2014). These upregulated miRNA have also been shown to impact mitochondrial structure and/or function: miR-140* via localization to the mitochondria for intrinsic apoptosis modulation and regulation of organellar fission (Li et al., 2012; Li et al., 2014); miR-17 via negative regulation of mitochondrial antioxidant enzyme levels (Du et al., 2014); and miR-16 via compromised mitochondrial integrity and mediation of mitochondria-dependent apoptosis (Li et al., 2012).

On the other hand, rno-miR-206, rno-miR-181a, rno-miR-138 and rno-miR-29c were significantly downregulated in *HMOX1*-transfected rat astrocytes compared to sham-transfected rat astrocytes (Lin et al., 2015). While mmu-miR-181a was significantly downregulated in TG STM compared to WT STM and mmu-miR-206 was significantly downregulated in primary TG astrocytes co-cultured with primary TG neurons compared to WT preparations, the remainder of these miRNA expression levels were either not significantly altered or significantly upregulated in TG samples compared to WT controls (Table 4; Table 5). MiR-181a and miR-206 are part of the large miRNA networks that are regulated by oxidative stress (Pizzimenti et al., 2009; Hutchinson et al., 2013; Ma et al., 2013; Wang et al., 2014). Furthermore, the concomitant decline of miR-181a and miR-206 expression levels in TG samples may either endanger or protect the mitochondrial compartment. MiR-181a is also involved in macroautophagy regulation via targeting of ATG5-12 (Frankel and Lund, 2012; Tekirdag et al., 2013). Fittingly, mitochondrial abnormalities have been amply documented in

human PD and other neurodegenerative disorders (Hattori et al., 1991; Bowen et al., 1995; Hirai et al., 2001; Storm et al., 2002; Exner et al., 2012).

The Dopaminergic System

At its core, PD is a neurodegenerative disease with early prominent death of DA neurons in the SN and STM of the basal ganglia, ultimately leading to a movement disorder characterized by classical parkinsonian motor symptoms (Kalia and Lang, 2015). Genes involved in DA metabolism and uptake, TH and DAT, as well as genes involved in DA neuron synthesis and survival, Nurr1, Pitx3 and LMX1B, were significantly downregulated in TG STM as well as neurons co-cultured with TG astrocytes compared to WT control preparations (Figure 3A, B). Furthermore, TH and DAT protein levels were also significantly decreased in TG neurons co-cultured with TG astrocytes compared to WT preparations (Figure 3C, D). Interestingly, WT and TG neurons grown alone, with virtually no glial contact, resulted in no significant differences in TH or DAT protein expression levels (Figure 3C, D). This highlights the importance of glial *HMOX1* overexpression on the resultant neuronal dysfunction. Although the underlying mechanism of DA degeneration in PD remains unknown, this glial HO-1 response may represent a pivotal transducer of noxious environmental and endogenous stressors into patters of neural damage characteristic of PD and other human degenerative CNS disorders (Schipper and Song, 2015).

Both mmu-miR-133b and mmu-miR-145 were significantly upregulated in the STM of GFAP.HMOX1$^{8.5\text{-}19m}$ mice compared to WT controls, as well as in TG astrocyte and neuron co-cultures compared to WT preparations (Figure 3E, F), correlating to the downregulation of their targets, Pitx3 and Nurr1 respectively, in these samples.

Deregulation of expression levels of these miRNAs may contribute to pathogenesis of PD, as the miR-133b-Pitx3 and miR-145-Nurr1 feedback loop is essential for maintaining viability and function of DA neurons in the brain (Kim et al., 2007).

Protein Aggregation

Alpha-synuclein, a key player in Lewy body formation in PD, was significantly upregulated at the mRNA and protein expression level in the parkinsonian GFAP.HMOX1$^{8.5\text{-}19m}$ mouse model compared to WT controls (Figure 4A, C; Figure 5; Figure 6). This is consistent with alpha-synuclein mRNA and protein expression levels observed in the basal ganglia of human PD subjects (Baba et al., 1998; Grundemann et al., 2008). Furthermore, the apparent increase in both intracellular and extracellular alpha-synuclein as shown by immunofluorescence (Figure 5), lends support to the recent prion hypothesis of alpha-synuclein propagation (Luk et al., 2012), while the increase in the tetrameric form of alpha-synuclein in primary TG neurons co-cultured with TG astrocytes compared to WT preparations suggests that alpha-synuclein is oligomerizing in the aging GFAP.HMOX1 mouse model. As such, the mechanism of alpha-synuclein propagation merits further investigation in this parkinsonian model system.

Several miRNAs, including miR-7a, miR-7b, miR-153 and miR-223, have been implicated in the regulation of alpha-synuclein mRNA expression levels (Doxakis, 2010; Junn et al., 2009). Two of the four miRNAs targeting alpha-synuclein, namely mmu-miR-153 and mmu-miR-223, were significantly downregulated in the SN and STM of TG mice compared to WT controls (Figure 4D). Downregulation of mmu-miR-153 and mmu-miR-223 may lead to the upregulation of alpha-synuclein mRNA and protein observed in

aging GFAP.HMOX1$^{8.5\text{-}19m}$ mice. A similar pattern was observed *in vitro*, in which both 3-day primary TG astrocyte and neuron co-cultures also displayed significant downregulation of mmu-miR-153 and mmu-miR-223 (Figure 4E), recapitulating miRNA expression levels observed *in vivo*. Together, these findings strongly suggest that down-modulation of mmu-miR-153 and mmu-miR-223 is responsible for up-regulation of alpha-synuclein mRNA in the brains of GFAP.HMOX1$^{8.5\text{-}19m}$ mice. On the other hand, the contribution of the mmu-miR-7 family to the regulation of alpha-synuclein mRNA in our model may be little or nil because (i) the opposing cell-specific changes in mmu-miR-7a and mmu-miR-7b observed in cultured astrocytes and neurons on *in vitro* day 3 may have attenuated any measurable change in mmu-miR-7a and mmu-miR-7b expression *in vivo* and (ii) there were no significant changes in glial or neuronal mmu-miR-7b expression at 7 days *in vitro*. Primary TG astrocytes grown in co-culture for 7 days, on the other hand, exhibited upregulation of miR-153 and no change in miR-223 (Figure 4F). This supports the notion that miRNAs are highly stable and accumulate over time, as mature miRNAs persist for many hours or even days after their production is arrested (i.e. by transcriptional shut-down through chemical inhibitors or depletion of miRNA processing enzymes) (Lee et al., 2003; Van Rooj et al., 2007; Baccarini et al., 2011; Gantier et al., 2011).

In contradistinction to the current data set, the GFAP.HMOX1$^{0\text{-}12m}$ developmental mouse model of schizophrenia, in which the *HMOX1* transgene is induced during neuroembryogenesis and the first 12 months of life, displayed significantly decreased expression of miR-7b associated with increased expression of alpha-synuclein in the nigrostriatum (Song et al., 2012). Together, these observations indicate that the

involvement of miR-7b in the regulation of alpha-synuclein may differ substantially among various disease states. Our findings raise the possibility that alpha-synuclein expression in neurodevelopmental conditions, e.g. schizophrenia, is largely controlled by miR-7b, whereas in neurodegenerative disorders, such as PD, the influences of miR-153 and miR-223 predominate. Alternatively, the 'switch' in miRNA regulation of neural alpha-synuclein expression may be a normal, aging-dependent phenomenon unrelated to specific disease states. In support of the latter, changes in miRNA expression patterns over the course of normal aging have been documented in other animal models (Lukiw, 2007; Hooten et al., 2010; Somel et al., 2010).

Alpha-synuclein is further regulated by the lysosomal proteases CtsB and CtsD (Lopes da Fonseca et al., 2015) and Notch1. Deficient CtsB and CtsD function promotes alpha-synuclein aggregation and lysosomal dysregulation, leading to alpha-synuclein toxicity (Cullen et al., 2009; Lopes da Fonseca et al., 2015). Similarly, CtsB and CtsD mRNA were found to be significantly downregulated in the SN and STM of TG mice compared to WT controls (Figure 4B). The Notch signaling pathway, on the other hand, is involved in regulating cell fate, proliferation and homeostasis (Baek et al., 2015). Alpha-synuclein has been previously shown to promote degradation of Notch1 intracellular domain through the ubiquitin E3 ligase, Fbw7 (Baek et al., 2015). Notch1 mRNA was significantly downregulated in the SN of TG mice compared to WT controls, with no significant change observed in the STM (Figure 4B).

In conclusion, the data obtained regarding alpha-synuclein expression in the GFAP.HMOX1$^{8.5\text{-}19m}$ mouse model is reminiscent of human PD pathology. The presence of Lewy bodies, largely composed of aggregated alpha-synuclein fibrils and

oligomers, is a histological hallmark of PD (Lewy, 1912; Polymeropoulos et al., 1997; Parent and Parent, 2010). While the exact mechanism of Lewy body formation remains unclear, studies of their topographic distribution during the course of sporadic PD has enabled a classification of the stages of disease progression to be drawn up (Braak et al., 2003). Furthermore, the recent prion hypothesis sheds light on alpha-synuclein propagation in PD brains (Luk et al., 2012; Giraldez-Perez et al., 2014; Chu and Kordower, 2015). Although, inclusion bodies were not observed in GFAP.HMOX1$^{8.5\text{-}19m}$ mice, this pathology may be observed later in disease progression, beyond 19 months of age, as discussed further below.

Oxidative Stress

Among the genes involved in oxidative stress modulation, MnSOD mRNA was significantly upregulated in TG STM and SN, as well as primary TG astrocyte and neuron co-cultures, compared to WT control preparations (Figure 7A, B). This is consistent with previous findings showing MnSOD accumulation in cultured astrocytes under HO-1 provocation (Frankel et al., 2000) and in the SN of human PD subjects (Saggu et al., 1989). The induction of MnSOD in the PD brain may be beneficial by curtailing superoxide toxicity within the mitochondrial compartment. Alternatively, MnSOD overexpression may exacerbate oxidative neural injury by promoting the accumulation of superoxide-derived hydrogen peroxide if enzymes mediating the removal of the latter (e.g. catalase, glutathione peroxidase) are limiting (the “SOD paradox”). Corroborating the mRNA data, MnSOD protein was also significantly increased in SN of GFAP.HMOX1$^{8.5\text{-}19m}$ mice compared to WT preparations (Figure 8).

PGC1a, a positive regulator of the genes required for mitochondrial biogenesis and the cell's antioxidant responses, was also significantly upregulated in TG STM and SN, as well as primary TG astrocyte and neuron co-cultures, compared to WT control preparations (Figure 7A, B). This upregulation is likely in response to the increased levels of ambient oxidative stress in the GFAP.HMOX1 mice (Song et al., 2012). On the other hand, Sirt1 mRNA was significantly upregulated in SN and downregulated in STM, while Parp1 mRNA was downregulated in STM as well, yet unchanged in STM compared to WT controls (Figure 7A). *In vitro*, Sirt1 and PARP1 mRNAs were significantly upregulated in both TG neuron and TG astrocyte primary co-cultures (Figure 7B). Sirt1 is known to protect against oxidative damage and protein misfolding (Donmez et al., 2012), two hallmark features of PD, which may explain the apparent upregulation of Sirt1 mRNA in aging GFAP.HMOX1$^{8.5\text{-}19m}$ mice. However, the downregulation of Sirt1 mRNA observed in TG STM suggests dysfunction of this protective mechanism. PARP1, on the other hand, is activated by DNA damage, and its overexpression has been previously associated with the pathogenesis of numerous CNS disorders, including ischemia, neuroinflammation and neurodegeneration (Martire et al., 2015).

Sirt1 is a putative target of miR-128. Mmu-miR-128-1-5p was downregulated in TG SN compared to WT controls (Figure 7C), correlating inversely with the observed upregulation of Sirt1 mRNA is TG SN. However, *in vitro* results did not correlate inversely with Sirt1 mRNA expression levels.

Mitochondrial Dysfunction

In PD-affected brain tissues, weakened mitochondria may represent both sources and chief targets of the excess ROS, as indicated by (i) diminished cytochrome subunit expression and complex I activity (Hattori et al., 1991); (ii) oxidative mitochondrial DNA lesions in neurons and astroglia (Storm et al., 2002); and (iii) suppressed glucose utilization and augmented lactate production *in vivo* (Bowen et al., 1995). Mitochondrial dysfunction has been previously reported in *HMOX1*-transfected rat astrocytes (Zukor et al., 2009), as well as in the brains of GFAP.HMOX1 mice (Song et al., 2012). Mitochondrial dysfunction was evaluated in aging GFAP.HMOX1$^{8.5\text{-}19m}$ mice in terms of apoptosis, autophagy – mitophagy – and mitochondrial biogenesis.

Apoptosis

Several genes involved in mitochondria-dependent apoptosis, including p53, p21, PUMA, Bak, Bax and Bcl2, were analyzed and found to be significantly upregulated at the mRNA level in both TG STM and SN compared to WT controls (Figure 9A). These results were recapitulated *in vitro*, with the exception of p53 mRNA in primary neurons co-cultured with primary TG astrocytes, which was significantly downregulated (Figure 9B). The role of apoptosis in PD pathology has been studied extensively and confirmed in human tissue postmortem by TUNEL staining (Tatton et al., 2003) and by increased immunostaining for caspase-3, caspase-8 and caspase-9 in nigrostriatal DA neurons (Hartmann et al., 2000; Tatton, 2000). Likewise, in the present study, the active form of caspase-3 was significantly increased in TG neurons co-cultured with TG astrocytes compared to WT preparations (Figure 9C). Apoptotic protein machinery was analyzed further using FACS, which measures early and late stage apoptosis in live cells. In

primary TG astrocytes co-cultured with TG neurons, early stage apoptosis was increased while late stage apoptosis was decreased (Figure 10A). In primary TG neurons co-cultured with TG astrocytes, there was no significant difference in early stage apoptosis, however these neurons exhibited increased late stage apoptosis compared to WT controls (Figure 10B). This is similar to a result published by our group previously, in which PC12 neuronal cells grown atop *HMOX1*-transfected astrocytes, but not the astrocytes themselves, were significantly more susceptible to oxidant-mediated cell death relative to control preparations (Song et al., 2007). The capacity of stressed astroglia to mount robust antioxidant defenses, upregulate cytoprotective heat shock proteins and adapt to anaerobic metabolism may account for persistence of these cells in degenerating human CNS in face of concomitant neuronal depletion (Schipper, 2004).

Several miRNAs were selected as potential regulators of genes involved in mitochondria-dependent apoptosis, including miR-153, miR-208a-3p and miR-208b, targeting p21, miR-200c-3p, targeting the apoptotic pathway as a whole, and miR-325, targeting p53 (www.targetscan.org). The majority of these miRNA were significantly downregulated *in vivo* and *in vitro*, correlating inversely to the upregulation observed in genes encoding apoptotic machinery and supporting the possible regulatory role of these miRNAs in the apoptotic pathway (Figure 9D, E).

Autophagy and Mitophagy

BECN1, Lamp2, p62 and Hdac6, genes involved in the autophagic pathway, were significantly upregulated at the mRNA level in both *in vivo* and *in vitro* samples from the GFAP.HMOX mouse compared to WT controls (Figure 11A, B). Increased

macroautophagy has been previously shown in *HMOX1*-transfected rat astrocytes, as well as in GFAP.HMOX1 mice (Zukor et al., 2009; Song et al., 2012). In addition, the ratio of LC3B-II to LC3B-I was analyzed in order to assess the level of autophagy at the protein level. The autophagic machinery was significantly increased in TG astrocytes co-cultured with TG neurons, consistent with previous findings, however the TG neurons co-cultured with TG astrocytes displayed a significant decrease in the autophagic machinery (Figure 11C). These findings indicate robust dysregulation of the autophagic system in the brains of GFAP.HMOX1 mice.

Furthermore, p62 is a putative target of mmu-miR-325, which was significantly downregulated in TG SN and STM as well as TG astrocytes co-cultured with TG neurons (Figure 14C, D). These findings correlate inversely with the apparent upregulation of p62 mRNA *in vivo* and *in vitro*, suggesting a possible regulatory role of miR-325 in the autophagic pathway.

Defects in mitophagy, the process that entails the clearance of mitochondria from cells via autophagy, have been implicated in the accumulation of protein aggregates and formation of inclusion bodies in surviving neurons (Hara et al., 2006; Komatsu et al., 2006; Deas et al., 2011). In GFAP.HMOX1, the genes involved in mitophagy, specifically parkin, PINK1, PTEN, were significantly upregulated both TG SN and in primary co-cultures (Figure 12A, B). There appears to be a dysregulation in the mitophagic system as an accumulation of dystrophic mitochondria is observed via TEM in TG STM (unpublished data), suggesting the genes involved in this pathway may be upregulated as a compensatory mechanism, yet protein translation may not be occurring or the extent of mitochondrial damage overwhelms the mitophagic machinery.

Another gene, DJ-1, involved in mitophagy – in addition to transcriptional regulation, antioxidative stress reaction, and chaperone, protease and mitochondrial regulation – was significantly downregulated in both *in vivo* and *in vitro* samples from GFAP.HMOX1 mice (Figure 12A, B). Interestingly, this gene has been implicated in both familial and sporadic PD and other neurodegenerative conditions, as excessive oxidized DJ-1, its inactive form, has been observed in brains of patients with PD and AD (Bandopadhyay et al., 2004; Choi et al., 2006; Ariga et al., 2013). Moreover, DJ-1 knockout mice exhibit key parkinsonian features, including motor impairment and altered DA function in the nigrostriatal pathway (Harvey et al., 2009; Lopert and Patel, 2014). Mutations in parkin, PINK1 and DJ-1 have been linked to early onset PD (Harvey et al., 2009).

Mitochondrial Biogenesis

The mitochondrial fission and fusion system plays an important role by sorting out damaged mitochondrial components and fragments as well as isolating defective mitochondria prior to mitophagy. Fusion is the combination of two mitochondria into a single organelle, while fission is the separation of long, tubular mitochondria into two or more smaller parts (Arduino et al., 2011). Imbalance of this system leads to tissue histopathology, as seen in PD. In GFAP.HMOX1$^{8.5\text{-}19m}$ mice, Mfn1, Mfn2 and OPA-1 mRNA, three pivotal mitochondrial fusion proteins, are significantly upregulated in the SN and STM, while Drp1, a mitochondrial fission protein, was significantly downregulated in both brain regions compared to WT preparations (Figure 13A). While these data were not recapitulated *in vitro* (Figure 13B), it is clear that there is an imbalance in the genes involved in mitochondrial biogenesis, ultimately suggesting dysregulation of this system.

Reelin

The neuronal and extracellular matrix glycoprotein, reelin, is best known for its function in the organization of cytoarchitectonics and regulation of synaptic plasticity in the developing CNS. In the TG mouse model of schizophrenia, GFAP.HMOX1$^{0\text{-}12m}$, neuronal reelin content was significantly diminished, consistent with reelin observations in human schizophrenia patients (Knuesel, 2010; Song et al., 2012). Its function in the adult brain, on the other hand, is less well understood, but it is conjectured to play an important role in learning and memory through maintenance of long-term potentiation, as well as being involved in signaling pathways linked to neurodegeneration (Botella-Lopez et al., 2006). Interestingly, reelin and GAD67 mRNA levels (the latter acting downstream of reelin) were significantly upregulated in both *in vivo* and *in vitro* samples from GFAP.HMOX1$^{8.5\text{-}19m}$ mice (Figure 14A, B). While the reelin pathway has not been extensively studied in regard to neurodegenerative disorders, one group found significantly elevated levels of reelin in the cerebrospinal fluid of PD and AD patients (Botella-Lopez et al., 2006).

Reelin is a putative target of mmu-miR-200c-3p (Stary et al., 2015), which was significantly downregulated in TG STM and TG neurons co-cultured with TG astrocytes, suggesting a possible regulatory role of this miRNA in the reelin pathway (Figure 14C, D). Compensatory reelin induction may augment synaptic plasticity in PD-affected neural tissues and possibly serve as a useful biomarker of the disease.

Significance

By 2030, the number of people living with neurodegenerative disorders, like PD, is expected to increase by 50%. In addition to the disability that ensues for sufferers of

PD, the patient's primary caregiver also carries a physically, emotionally and financially demanding burden. With solely symptomatic and no curative treatments currently available for PD, advances in this field of research are imperative for the near future. The Schipper laboratory has made significant advances in the neurodegenerative field in recent years with the advent of the GFAP.HMOX1$^{8.5\text{-}19m}$ TG mouse model of PD. The current research project has helped to further characterize this model and better understand the role of HO-1 in neurodegeneration in order to pave the path toward identification of new therapeutic targets for the management of PD.

It cannot be denied that HO-1 elicits neuroprotection under certain circumstances. Relative cytoprotection has been reported in *HMOX1*-transfected neuroblastoma cells following exposure to hydrogen peroxide (Le et al., 1999; Takeda et al., 2000) or beta-amyloid (Le et al., 1999). Similarly, HO-1 transgenic mice subjected to cerebral ischemia (Panahian et al., 1999), brain or spinal cord trauma (Fukuda et al., 1996; Lin et al., 2007) or excitotoxin exposure (Huang et al., 2005; Ahmad et al., 2006) exhibit smaller infarct sizes and lower biochemical indices of neural injury. These examples highlight the cytoprotective nature of HO-1 in acute models of CNS disease and injury. Chronic overexpression of glial HO-1, on the other hand, is predominantly detrimental to neural tissues (Schipper and Song, 2015).

The data presented herein indicate that astroglial HO-1 is well positioned to transduce a host of noxious stimuli and risk factors into 'core' neuropathology common to PD and other aging-related neurodegenerative disorders. This is also highlighted by the co-culture experiments, where primary astrocytes and neurons were individually isolated from both WT and TG GFAP.HMOX1$^{8.5\text{-}19m}$ mice. In this aging model, *HMOX1*

is selectively overexpressed in the astrocytic compartment, meaning the neurons are not genetically manipulated in any way. However, when grown in co-culture with TG GFAP.HMOX1 primary astrocytes, changes in miRNA and mRNA expression levels are noted in the neurons. Glial cells serve as support cells to neurons in the brain, and overexpression of HO-1 in the astrocytes is significantly impacting the structure and function of neurons both *in vivo* and *in vitro*, ultimately leading, in the case of aging GFAP.HMOX1$^{8.5\text{-}19m}$ mice, to neuropathological and behavioural changes reminiscent of human idiopathic PD.

Future Studies

Future work will entail a mechanistic study of the role(s) of specific miRNA (miR-153 and miR-223) in the regulation of alpha-synuclein expression and ensuing PD pathology. This will be assessed in two ways: 1) Employing specific miRNA mimics and/or inhibitors on human neuroblastoma cell lines (BE(2)-M17 and SH-5YSY). This post-transcriptional gene silencing mechanism uses double stranded RNA as a signal to trigger degradation of homologous mRNA via siRNAs (Elbashir et al., 2002). It has been proposed that the interaction between Dicer and Ago2 facilitates siRNA incorporation into RISC (Elbashir et al., 2002); thus, 2) analyzing the recruitment of miRNAs and mRNAs to RISC by Dicer and Ago2 co-immunoprecipitation. Biological actions of miRNA require cytoplasmic processing by Dicer, interaction with Ago2 proteins and assembly into RISC, which promotes and stabilizes miRNA base pair annealing with the target mRNA (Wang et al., 2015). Dicer and Ago2 are present in mitochondrial fractions from normal mammalian brain, and immunoprecipitation of Ago2-associated miRNA from mitochondria suggests the presence of functional RISC (Wang et al., 2015). This

experiment will validate select miRNA expression level data, ensuring that the regulatory machinery is either present (upregulated) or not present (downregulated). These techniques will help better understand the potential role of endogenous miRNAs in regulation and dysregulation of mammalian alpha-synuclein gene function in PD pathogenesis.

Additionally, the parkinsonian GFAP.HMOX1 mouse model will be utilized in order to assess the mechanism of alpha-synuclein propagation in mammals (Luk et al., 2012; Giraldez-Perez et al., 2014; Chu and Kordower, 2015). Based on evidence discussed above, we suspect alpha-synuclein may be propagating within the brain in a manner that is similar to prion proteins, as recently proposed by Trojanowski and others (Luk et al., 2012; Giraldez-Perez et al., 2014; Chu and Kordower, 2015). We anticipate that alpha-synuclein propagation and possibly inclusion body formation will be enhanced in the GFAP.HMOX1 mouse due to increased levels of oxidative stress and autophagic dysregulation.

Finally, a priority issue in contemporary neurobiology concerns the degree of reversibility of CNS damage, via indigent repair mechanisms and neuroplasticity, after offending stimuli have dissipated (Schipper, 2015). Spontaneous remission of both neurodegenerative pathology and associated behavioural abnormalities occurred in certain conditional transgenic mouse models following experimental suppression of the mutant transgene, including APP TG mouse models of AD (Kotilinek et al., 2002), mutant tau-driven models of AD and frontotemporal dementia (Sydow et al., 2011), the MPTP mouse model of PD (Schmidt and Ferger, 2001), rodent models of Huntington disease (Yamamoto et al., 2000) and several spinocerebellar degeneration mimics (Boy

et al., 2009). Based on the restorative properties of the degenerating CNS adduced from the afore cited animal models, clinically relevant neuroregeneration may be invoked in a broad spectrum of neurodegenerative disorders following interruption of the salient pathological pathways (Schipper, 2015). We would like to ascertain the extent to which re-introduction of dietary DOX at 19 months of age enables the *reversal* of behavioural deficits and neuropathology in 24-month old GFAP.HMOX1 mice relative to age-matched control groups which were only exposed to DOX between 8.5 and 19 months of age.

Positive results in this tier of experiments would help to further unify several seemingly disparate pathological features of PD, including oxidative stress, iron mobilization, mitochondrial insufficiency and macroautophagy, into a single 'lesion' arising from the action of HO-1 within the astroglial compartment. Although we do not regard aberrant HO-1 expression as a 'cause' of PD, we view glial HO-1 hyperactivity as a pivotal transducer that funnels an array of noxious stimuli through limited neurodegenerative pathways culminating in nigrostriatal injury. HO-1 may therefore serve as an appropriate therapeutic target in PD patients, seeing as contemporary pharmacotherapy for PD is almost exclusively symptomatic. Metalloporphyrin inhibitors of HO activity are already in clinical use for the treatment of neonatal hyperbilirubinemia (jaundice) and certain adult liver conditions, and therefore could be adapted for the treatment of PD. OB-28 is a small-molecule inhibitor that is selective for HO-1 over HO-2, crosses the blood-brain barrier and has a favourable toxicity profile. In pre-clinical studies, treatment with OB-28 reduced oxidative damage to whole-cell and mitochondrial compartments in rat *HMOX1*-transfected astrocytes (Gupta et al., 2014).

Moreover, OB-28 was found to significantly counter behavioural deficits and neuropathological alterations in the $APP_{swe}/PS1_{\Delta E9}$ mouse model of AD (Gupta et al., 2014). Human clinical trials with OB-28 at strategic time points are merited in order to elucidate the effectiveness of glial HO-1 inhibition in the treatment of degenerative and/or developmental brain disease.

In conclusion, the advent of conditional GFAP.HMOX1 TG mice endows the biomedical community with a robust resource to investigate definitively the roles of glial stress and HO-1 in brain aging, PD – as shown in the current study – and other neurological afflictions, both adult and pediatric.

REFERENCES

1. Abbott, R. D., Ross, G. W., White, L. R., Sanderson, W. T., Burchfield, C. M., Kashon, M., Sharp, D. S., Masaki, K. H., Curb, J. D., and Petrovitch, H. (2003). Environmental, life-style, and physical precursors of clinical Parkinson's disease: recent findings from the Honolulu-Asia Aging Study. *Journal of Neurology,* 250(3), iii30-iii39.
2. Ahmed, A. S., Zhuang, H., and Dore, S. (2006). Heme oxygenase-1 protects brain from acute excitotoxicity. *Neuroscience*, 141, 1703-1708.
3. Alam, Z. I., Jenner, A., Daniel, S. E., Lees, A. J., Cairns, N., Marsden, C. D., Jenner P., and Halliwell, B. (1997). Oxidative DNA damage in the Parkinsonian brain: An apparent selective increase in 8-hydroxyguanine levels in the substantia nigra. *Journal of Neurochemistry,* 69(3), 1196-1203.
4. Albin, R. L., Young, A. B., and Penney, J. B. (1989). The functional anatomy of basal ganglia disorders. *Trends in Neuroscience,* 12(10), 366-375.
5. Angot, E., and Brundin, P. (2009). Dissecting the potential molecular mechanisms underlying alpha-synuclein cell-to-cell transfer in Parkinson's disease. *Parkinsonism and Related Disorders*, 3, S143-S147.
6. Angot, E., Steiner, J. A., Hansen, C., Li, J. Y., and Brundin, P. (2010). Are synucleinopathies prion-like disorders? *Lancet Neurology*, 9(11), 1128-1138.
7. Arduino, D. M., Esteves, A. R., and Cardoso, S. M. (2011). Mitochondrial fusion/fission, transport and autophagy in PD: when mitochondria get nasty. *Parkinson's Disease*, 2011.

8. Ariga, H., Takahashi-Niki, K., Kato, I., Maita, H., Takeshi, N., and Iguchi-Ariga, S. M. M. (2013). Neuroprotective function of DJ-1 in Parkinson's disease. *Oxidative Medicine and Cellular Longevity,* 2013, 1-9.
9. Baba, M., Nakajo, S., Tu, P. H., Tomita, T., Nakaya, K., Lee, V. M., Trojanowski, J. Q., and Iwatsubo, T. (1998). Aggregation of alpha-synuclein in Lewy bodies of sporadic Parkinson's disease and dementia with Lewy bodies. *American Journal of Pathology*, 152, 879-884.
10. Baccarini, A., Chauhan, H., Gardner, T. J., Jayaprakash, A. D., Sachidanandam, R., and Brown, B. D. (2011). Kinetic analysis reveals the fate of a microRNA following target regulation in mammalian cells. *Current Biology*, 21(5), 369-376.
11. Baek, H. J., Yoon, J. H., Ann, E. J., Kim, M. Y., Ahn, J. S., Kim, S. H., Jo, E. H., Lee, H. J., and Park, H. S. (2015). Alpha-synuclein negatively regulates Notch1 intracellular domain protein stability through promoting interaction with Fbw7. *Neuroscience Letters*, 600, 6-11.
12. Bandopadhyay, R. Kingsbury, A. E., Cookson, M. R., Reid, A. R., Evans, I. M., Hope, A. D., Pittman, A. M., Lashley, T., Canet-Aviles, R., Miller, D. W., McLendon, C., Strand, C., Leonard, A. J., Abou-Sleiman, P. M., Healy, D. G., Ariga, H., Wood, N. W., de Silva, R., Revesz, T., Hardy, J. A., and Lees, A. J. (2004). The expression of DJ-1 (PARK7) in normal human CNS and idiopathic Parkinson's disease. *Brain*, 127(2), 420-430.
13. Bartel, D. P. (2004). MicroRNAs: target recognition and regulatory functions. *Cell,* 136(2), 215-233.

14. Beal, M. F. (1995). Aging, energy, and oxidative stress in neurodegenerative diseases. *Annals of Neurology,* 38(3), 357-366.
15. Beninger, R. J. (1983). The role of dopamine in locomotor activity and learning. *Brain Research Reviews*, 6(2), 173-196.
16. Berardelli, A., Rothwell, J. C., Thompson, P. D., and Hallett, M. (2001). Pathophysiology of bradykinesia in Parkinson's disease. *Brain,* 124(11), 2131-2146.
17. Bergeron, M., Ferriero, D. M., and Sharp, F. R. (1998). Developmental expression of heme oxygenase-1 (HSP32) in rat brain: an immunocytochemical study. *Developmental Brain Research,* 105(2), 181-194.
18. Bifsha, P., Yang, J., Fisher, R. A., and Drouin, J. (2014). *Rgs6* is required for adult maintenance of dopaminergic neurons in the ventral substantia nigra. *PLOS Genet,* 10(12), e1004863.
19. Boissonneault, V., Plant, I., Rivest, S., and Provost, P. (2009). MicroRNA-298 and microRNA-328 regulate expression of mouse beta-amyloid precursor protein-converting enzyme 1. *Journal of Biological Chemistry,* 284(4), 1971-1981.
20. Botella-Lopez, A., Burgaya, F., Gavin, R., Garcia-Ayllon, M. S., Gomez-Tortosa, E., Pena-Casanova, J., Urena, J. M., Del Rio, J. A., Blesa, R., Soriano, E., and Saez-Valero, J. (2006). Reelin expression and glycosylation patterns are altered in Alzheimer's disease. *Proceedings of the National Academy of Sciences*, 103(14), 5573-5578.
21. Bowen, B. C., Block, R. E., Sanchez-Ramos, J., Pattany, P. M., Lampman, D. A., Murdoch, J. B., and Quencer, R. M. (1995). Proton MR spectroscopy of the brain

in 14 patients with Parkinson disease. *American Journal of Neuroradiology*, 16, 61-68.

22. Boy, J., Schmidt, T., Wolburg, H., Mack, A., Nuber, S., Bottcher, M., Schmitt, I, Holzmann, C., Zimmermann, F., Servadio, A., and Riess, O. (2009). Reversibility of symptoms in a conditional mouse model of spinocerebellar ataxia type 3. *Human Molecular Genetics*, 18, 4282-4295.
23. Braak, H., Del Tredici, K., Rub, U., de Vos, R. A., Steur, E. N. J., and Braak, E. (2003). Staging of brain pathology related to sporadic Parkinson's disease. *Neurobiology of Aging*, 24(2), 197-211.
24. Brichta, L., Greengard, P., and Flajolet, M. (2013). Advances in the pharmacological treatment of Parkinson's disease: targeting neurotransmitter systems. *Trends in Neuroscience,* 36(9), 543-554.
25. Castellani, R., Smith, M. A., Richey, P. L., Kalaria, R., Gambetti, P., and Perry, G. (1995). Evidence for oxidative stress in Pick disease and corticobasal degeneration. *Brain Research*, 696(1), 268-271.
26. Celardo, I., Martins, L. M., and Gandhi, S. (2014). Unraveling mitochondrial pathways to Parkinson's disease. *British Journal of Pharmacology,* 171(8), 1943-1957.
27. Charcot, J. M. (1872). De la paralysie agitante. In Oeuvres Completes (t 1) Lecons sur les maladies du systeme nerveux, pp. 115 – 188 A Delahaye, Paris: [In English: Charcot, J. M. (1877). On Parkinson's disease. In *Lectures on diseases of the nervous system delivered at the Salpetriere* (transl. Sigerson G), pp. 129 – 156. New Sydenham Society, London.]

28. Chaudhuri, K. R., Healy, D. G., Schapira, A. H. (2006). Non-motor symptoms of Parkinson's disease: diagnosis and management. *The Lancet Neurology,* 5(3), 235-245.
29. Chen-Roetling, J., Song, W., Schipper, H. M., Regan, C. S., and Regan, R. F. (2015). Astrocyte overexpression of heme oxygenase-1 improves outcome after intracerebral hemorrhage. *Stroke*, 46(4), 1093-1098.
30. Chinta, S. J., Andersen, J. K. (2005). Dopaminergic neurons. *The International Journal of Biochemistry and Cell Biology,* 37(5), 942-946.
31. Choi, J., Sullards, M. C., Olzmann, J. A., Rees, H. D., Weintraub, S. T., Bostwick, D. E., Gearing, M., Levey, A. I., Chin, L. S., and Li, L. (2006). Oxidative damage of DJ-1 is linked to sporadic Parkinson and Alzheimer diseases. *Journal of Biological Chemistry*, 281(16), 10816-10824.
32. Chopra, V. S., Moozar, K. L., Mehindate, K., and Schipper, H. M. (1997). A cellular stress model for the differential expression of glial lysosomal cathepsins in the aging nervous system. *Experimental Neurology,* 147(2), 221-228.
33. Chu, Y., and Kordower, J. H. (2015). The prion hypothesis of Parkinson's disease. *Current Neurology and Neuroscience Reports*, 15(5), 1-10.
34. Cookson, M. R., and van der Brug, M. (2008). Cell systems and the toxic mechanism(s) of alpha-synuclein. *Experimental Neurology,* 209 (1), 5-11.
35. Crossman, A. R. (1987). Primate models of dyskinesia: The experimental approach to the study of basal ganglia-related involuntary movement disorders. *Neuroscience,* 21(1), 1-40.

36. Cullen, V., Lindfors, M., Ng, J., Paetau, A., Swinton, E., Kolodziej, P., Boston, H., Saftig, P., Woulfe, J., Feany, M. B., Myllykangas, L., Schlossmacher, M. G., and Tyynela, J. (2009). Cathepsin D expression level affects alpha-synuclein processing, aggregation, and toxicity in vivo. *Molecular Brain*, 2, 5.
37. Deas, E., Wood, N. W., and Plun-Favreau, H. (2011). Mitophagy and Parkinson's disease: The PINK1-parkin link. *Biochimica et Biophysica Acta (BBA)-Molecular Cell Research,* 1813(4), 623-633.
38. DeLong, M. R. (1990). Primate models of movement disorders of basal ganglia origin. *Trends in Neurosciences,* 13(7), 281-285.
39. DeLong, M. R., and Wichmann, T. (2007). Circuits and circuit disorders of the basal ganglia. *Archives of Neurology*, 64(1), 20-24.
40. Dennery, P. A. (2000). Regulation and role of heme oxygenase in oxidative injury. *Current Topics in Cellular Regulation,* 36, 181-199.
41. Devi, L. Raghavendran, V., Prabhu, B. M., Avadhani, N. G., and Anandatheerthavarada, H. K. (2008). Mitochondrial import and accumulation of alpha-synuclein impair complex 1 in human dopaminergic neuronal cultures and Parkinson disease brain. *Journal of Biological Chemistry,* 283(14), 9089-9100.
42. Devos, D., Moreau, C., Devedjian, J. C., Kluza, J., Petrault, M., Laloux, C., Jonneaux, A., Ryckewaert, G., Garcon, G., Rouaix, N., Duhamel, A., Jissendi, P., Dujardin, K., Auger, F., Ravasi, L., Hopes, L., Grolez, G., Firdaus, W., Sablanniere, B., Strubi-Vuillaume, I., Zahr, N., Destee, A., Corvol, J. C., Poltl, D., Leist, M., Rose, C., Defebvre, L., Marchetti, P., Cebantchik, Z. I., Bordet, R.

(2014). Targeting chelatable iron as a therapeutic modality in Parkinson's disease. *Antioxidant and Redox Signaling,* 21(2), 195-210.

43. Dias, V., Junn, E., and Mouradian, M. M. (2013). The Role of Oxidative Stress in Parkinson's Disease. *Journal of Parkinson's Disease,* 3(4), 461-491.
44. Donmez, G., Arun, A., Chung, C. Y., McLean, P. J., Lindguist, S., and Guarente, L. (2012). SIRT1 protects against alpha-synuclein aggregation by activating molecular chaperones. *The Journal of Neuroscience,* 32(1), 124-132.
45. Doxakis, E. (2010). Post-transcriptional regulation of alpha-synuclein expression by miR-7 and miR-153. *Journal of Biological Chemistry*, 285(17), 12726-12734.
46. Du, W., W., Yang, W., Fang, L., Xuan, J., Li, H., Khorshidi, A., Gupta, S., Li, X., and Yang, B. B. (2014). MiR-17 extends mouse lifespan by inhibiting senescence signaling mediated by MKP7. *Cell Death and Disease*, 5, e1355.
47. Elbashir, S. M., Ahrborht, J., Weber, K., and Tuschl, T. (2002). Analysis of gene functions in somatic mammalian cells using small interfering RNAs. *Methods,* 26(2), 199-213.
48. Ewing, J. F., Haber, S. N., and Maines, M. D. (1992). Normal and heat-induced patterns of expression of heme oxygenase-1 (HSP32) in rat brain: hyperthermia causes rapid induction of mRNA and protein. *Journal of Neurochemistry*, 58(3), 1140-1149.
49. Exner, N., Lutz, A. K., Haass, C., and Winklhofer, K. F. (2012). Mitochondrial dysfunction in Parkinson's disease: molecular mechanisms and pathophysiological consequences. *EMBO Journal*, 31(14), 3038-3062.

50. Fatima, A., Lynn, D. J., O'Boyle, P., Seoighe, C., and Morris, D. (2014). The miRNAome of the postpartum dairy cow liver in negative energy balance. *BMC Genomics*, 15, 279.
51. Fearnley, J. M., and Lees, A. J. (1991). Ageing and Parkinson's disease: substantia nigra regional selectivity. *Brain,* 114(5), 2283-2301.
52. Fenton, H., Finch, P. W., Rubin, J. S., Rosenberg, J. M., Taylor, W. G., Kuo-Leblanc, V., Rodrigues-Wolf, M., Baird, A., Schipper, H. M., and Stopa, E. G. (1998). Hepatocyte growth factor (HGF/SF) in Alzheimer's disease. *Brain Research,* 779(1), 262-270.
53. Floor, E., and Wetzel, M. (1998). Increased protein oxidation in human substantia nigra pars compacta in comparison with basal ganglia and prefrontal cortex measured with an improved dinitrophenylhydrazine assay. *Journal of Neurochemistry,* 70(1), 268-275.
54. Frankel, D., Mehindate K., and Schipper, H. M. (2000). Role of heme oxygenase-1 in the regulation of manganese superoxide dismutase gene expression in oxidatively challenged astroglia. *Journal of Cellular Physiology*, 185, 80-86.
55. Frankel, L. B., and Lund, A. H. (2012). MicroRNA regulation of autophagy. *Carcinogenesis*, 33, 2018-2025.
56. Frost, B., and Diamond, M. L. (2010). Prion-like mechanisms in neurodegenerative diseases. *Nature Reviews in Neuroscience*, 11, 155-159.
57. Fukuda, K., Richmon, J. D., Sato, M., Sharp, F. R., Panter, S. S., and Noble, L. J. (1996). Induction of heme oxygenase-1 (HO-1) in glia after traumatic brain injury. *Brain Research*, 736(1), 68-75.

58. Gains, M. J., Roth, K. A., LeBlanc, A. C. (2006). Prion protein protects against ethanol-induced Bax-mediated cell death in vivo. *Neuroreport,* 17(9), 903-906.

59. Gantier, M. P., McCoy, C. E., Rusinova, I., Saulep, D., Wang, D., Xu, D., Irving, A. T., Behlke, M. A., Hertzog, P. J., Mackay, F., and Williams, B. R. (2011). Analysis of microRNA turnover in mammalian cells following Dicer1 ablation. *Nucleic Acids Research*, 39(13), 5692-5703.

60. Giraldez-Perez, R. M., Antolin-Vallespin, M., Munoz, M. D., and Sanchez-Capelo, A. (2014). Models of alpha-synuclein aggregation in Parkinson's disease. *Acta Neuropathologica Communications*, 2(1), 176-193.

61. Grudemann, J., Schlaudraff, F., Haeckel, O., and Liss, B. (2008). Elevated alpha-synuclein mRNA levels in individual UV-laser-microdissected dopaminergic substantia nigra neurons in idiopathic Parkinson's disease. *Nucleic Acids Research*, 36, e38.

62. Guidotti, A., Auta, J., Davis, J. M., Di-Giorgi-Gerevini, V., Dwivedi, Y., Grayson, D. R., Impagnatiello, F., Pandey, G., Pesold, C., Sharma, R., Uzunov, D., and Costa, E. (2000). Decrease in reelin and glutamic acid decarboxylase67 (GAD67) expression in schizophrenia and bipolar disorder: a postmortem brain study. *Archives of General Psychiatry,* 57(11), 1061-1069.

63. Gupta, A., Lacoste, B., Pistell, P. J., Ingram, D. K., Hamel, E., Alaoui-Jamali, M. A., Szarek, W. A., Vlahakis, J. Z., Jie, S., Song, W., and Schipper, H. M. (2014). Neurotherapeautic effects of novel HO-1 inhibitors in vitro and in a transgenic mouse model of Alzheimer's disease. *Journal of Neurochemistry,* 131(6), 778-790.

64. Hara, T., Nakamura, K., Matsui, M., Yamamoto, A., Nakahara, Y., Suzuki-Migishima, R., Yokoyama, M., Mishima, K., Saito, I., Okano, H., and Mizushima, N. (2006). Suppression of basal autophagy in neural cells causes neurodegenerative disease in mice. *Nature*, 441, 885-889.

65. Hartmann, A., Hunot, S., Michel, P. P., Muriel, M. P., Vyas, S., Faucheux, B. A., Mouatt-Prigent, A., Turmel, H., Sriniyasan, A., Ruberg, M., Evan, G. I., Agid, Y., and Hirsch, E. C. (2000). Caspase-3: A vulnerability factor and final effector in apoptotic death of dopaminergic neurons in Parkinson's disease. *Proceedings of the National Academy of Sciences*, 97(6), 2875-2880.

66. Harvey, B. K., Wang, Y., and Hoffer, B. J. (2009). Transgenic rodent models of Parkinson's disease (pp. 89-92). Springer Vienna.

67. Hashimoto, M., Hsu, L. J., Xia, Y., Takeda, A., Sisk, A., Sundsmo, M., and Masliah, E. (1999). Oxidative stress induces amyloid-like aggregate formation of NACP/alpha-synuclein in vitro. *Neuroreport,* 10(4), 717-721.

68. Hassler, R. (1938). Zur Pathologie der Paralysis Agitans und des posten-zephalitischen Parkinsonismus. *Journal of Psychological Neurology,* 48, 387-476.

69. Hattori, N., Tanaka, M., Ozawa, T., Mizuno, Y. (1991). Immunohistochemical studies on complexes I, II, III and IV of mitochondria in Parkinson's disease. *Annals of Neurology*, 30, 563-571.

70. Hawkes, C. H., Shephard, B. C., and Daniel, S. E. (1997). Olfactory dysfunction in Parkinson's disease. *Journal of Neurology, Neurosurgery and Psychiatry,* 62(5), 436-446.

71. Hirai, K., Aliev, G., Nunomura, A., Fujioka, H., Russell, R. L., Atwood, C. S., Johnson, A. B., Kress, Y., Vinters, H. V., Tabaton, M., Shimohama, S., Cash, A. D., Siedlak, S. L., Harris, P. L., Jones, P. K., Petersen, R. B., Perry, G., and Smith, M. A. (2001). Mitochondrial abnormalities in Alzheimer's disease. *The Journal of Neuroscience*, 21(9), 3017-3023.

72. Hooten, N. N., Abdelmohsen, K., Gorospe, M., Ejiogu, N., Zonderman, A. B., and Evans, M. K. (2010). MicroRNA expression patterns reveal differential expression of target genes with age. *PLoS One*, 5(5), e10724.

73. Hornykiewicz, O. (1988). Neurochemical pathology and the etiology of Parkinson's disease: Basic facts and hypothetical possibilities. *The Mount Sinai Journal of Medicine, New York,* 55(1), 11.

74. Howell, J. C., Chun, E., Farrell, A. N., Hur, E. Y., Caroti, C. M., Luvone, P. M., and Haque, R. (2013). Global microRNA expression profiling: Curcumin (diferuloylmethane) alters oxidative stress-reponsive microRNAs in human ARPE-19 cells. *Molecular Vision*, 19, 544-560.

75. Huang, E., Ong, W. Y., Go, M. L., and Garey, L. J. (2005). Heme oxygenase-1 activity after excitotoxic injury: immunohistochemical localization of bilirubin in neurons and astrocytes and deleterious effects of heme oxygenase inhibition on neuronal survival after kainate treatment. *The Journal of Neuroscience Research*, 80, 268-278.

76. Hughes, A. J., Daniel, S. E., Blankson, S., and Lees, A. J. (1993). A clinicopathologic study of 100 cases of Parkinson's disease. *Archives of Neurology,* 50(2), 140-148.

77. Hutchinson, E. R., Kawamoto, E. M., Taub, D. D., Lal, A., Abdelmohsen, K., Zhang, Y., Wood, W. H., Lehrmann, E., Camandola, S., Becker, K. G., Gorospe, M., and Mattson, M. P. (2013). Evidence for miR-181 involvement in neuroinflammmatory responses of astrocytes. *GLIA*, 61, 1018-1028.

78. Jankovic, J. (2008). Parkinson's disease: clinical features and diagnosis. *Journal of Neurology, Neurosurgery and Psychiatry,* 79(4), 368-376.

79. Jenner, P. (2003). Oxidative stress in Parkinson's disease. *Annals of Neurology,* 53(S3), S26-S38.

80. Jones, E. V., Cook, D., and Murai, K. K. (2012). A neuron-astrocyte co-culture system to investigate astrocyte-secreted factors in mouse neuronal development. *Astrocytes: Methods and Protocols,* 341-352.

81. Jost, W. H. (1997). Gastrointestinal motility problems in patients with Parkinson's disease. *Drugs and Aging* 10(4), 249-258.

82. Junn, E., Lee, K. W., Jeong, B. S., Chan, T. W., Im, J. Y., and Mouradian, M. M. (2009). Repression of α-synuclein expression and toxicity by microRNA-7. *Proceedings of the National Academy of Sciences,* 106(31), 13052-13057.

83. Kalia, L. V., and Lang, A. E. (2015). Parkinson's disease. *Lancet*, 386, 896-912.

84. Keeney, P. M., Xie, J., Capaldi, R. A., Bennett, J. P. (2006). Parkinson's disease brain mitochondrial complex I has oxidatively damaged subunits and is functionally impaired and misassembled. *The Journal of Neuroscience,* 26(19), 5256-5264.

85. Kim, J., Inoue, K., Ishii, J., Vanti, W. B., Voronov, S. V., Murchison, E., Hannon, G., and Abeliovich, A. (2007). A microRNA feedback circuit in midbrain dopamine neurons. *Science,* 317(5842), 1220-1224.

86. Kinobe, R. T., Vlahakis, J. Z., Vreman, H. J., Stevenson, D. K., Brien, J. F., Szarek, W. A., and Nakatsu, K. (2006). Selectivity of imidazole-dioxolane compounds for in vitro inhibition of microsomal haem oxygenase isoforms. *British Journal of Pharmacology,* 147(3), 307-315.

87. Kish, S. J., Shannak K., Hornykiewicz, O. (1988). Uneven pattern of dopamine loss in the striatum of patients with idiopathic Parkinson's disease. *New England Journal of Medicine,* 318(14), 876-880.

88. Kitamuro, T., Takahashi, K., Ogawa, K., Udono-Fujimori, R., Takeda, K., Furuyama, K., Nakayama, M., Sun, J., Fujita, H., Hida, W., Hattori, T., Shirato, K., Igarashi, K., and Shibahara, S. (2003). Bach1 functions as a hypoxia-inducible repressor for the heme oxygenase-1 gene in human cells. *Journal of Biological Chemistry,* 278(11), 9125-9133.

89. Knuesel, I. (2010). Reelin-mediated signaling in neuropsychiatric and neurodegenerative diseases. *Progressive Neurobiology*, 91(4), 257-274.

90. Komatsu, M., Waguri, S., Chiba, T., Murata, S., Iwata, J., Tanida, I., Ueno, T., Koike, M., Uchiyama, Y., Kominami, E., and Tanaka, K. (2006). Loss of autophagy in the central nervous system causes neurodegeneration in mice. *Nature*, 441-880-884.

91. Kordower, J. H., and Brundin, P. (2009). Propagation of host disease to grafted neurons: accumulating evidence. *Experimental Neurology*, 220, 224-225.

92. Kotilinek, L. A., Bacskai, B., Westerman, M., Kawarabayashi, T., Younkin, L., Hyman, B. T., Younkin, S., and Ashe, K. H. (2002). Reversible memory loss in a mouse transgenic model of Alzheimer's disease. *The Journal of Neuroscience*, 22, 6331-6335.

93. Lai, B. C., Marion, S. A., Teschke, K., and Tsui, J. K. (2002). Occupational and environmental risk factors for Parkinson's disease. *Parkinsonism and Related Disorders,* 8(5), 297-309.

94. Lansbury, P. T., and Lashuel, H. A. (2006). A century-old debate on protein aggregation and neurodegeneration enters the clinic. *Nature,* 443(7113), 774-779.

95. Le, W. D., Xie, W. J., and Appel, S. H. (1999). Protective role of heme oxygenase-1 in oxidative stress-induced neuronal injury. *The Journal of Neuroscience Research*, 56, 652-658.

96. Le, W., and Jankovic, J. (2013). Animal models of Parkinson's disease. In: Jankovic J. (ed.) Parkinson's disease: diagnosis, motor symptoms and non-motor features. Clinical Insights E-Book Series, Future Science Group, London, UK, 2013, pp. 115-136.

97. Le, W., Sayana, P., and Jankovic, J. (2014). Animal models of Parkinson's disease: A gateway to therapeutics?. *Neurotherapeutics,* 11(1), 92-110.

98. Lee, Y., Ahn, C., Han, J., Choi, H., Kim, J., Yim, J., Lee, J., Provost, P., Radmark, O., Kim, S., and Kim, V. N. (2003). The nuclear RNase III Drosha initiates microRNA processing. *Nature*, 425(6956), 415-419.

99. Lewy, F. H. (1912). "Paralysis agitans. I. Pathologische anatomie." *Handbunch der Neurologie*, 3(part 2), 920-933.

100. Li, J., Li, Y., Jiao, J., Wang, J., Li, Y., Qin, D., and Li, P. (2014). Mitofusin 1 is negatively regulated by microRNA 140 in cardiomyocyte apoptosis. *Molecular and Cellular Biology*, 34, 1788-1799.

101. Li, P., Jiao, J., Gao, G., and Prabhakar, B. S. (2012). Control of mitochondrial activity by miRNAs. *Journal of Cellular Biochemistry*, 113, 1104-1110.

102. Li, Y., Liu, W., Oo, T. F., Wang, L., Tang, Y., Jackson-Lewis, V., Zhou, C., Geghman, K., Bogdonov, M., Przedborski, S., Beal, M. F., Burke, R. E., Li, C. (2009). Mutant LRRK2(R1441G) BAC transgenic mice recapitulate cardinal features of Parkinson's disease. *Nature Neuroscience,* 12(7), 826-828.

103. Lin, S. H., Song, W., Cressatti, M., Zukor, H., Wang, E., and Schipper, H. M. (2015). Heme oxygenase-1 modulates microRNA expression in cultures astroglia: implications for chronic brain disorders. *GLIA,* 63(7), 1270-1284.

104. Lin, Y., Vreman, H. J., Wong, R. J., Tjoa, T., Yamauchi, T., and Noble-Haeusslein, L. J. (2007). Heme oxygenase-1 stabilizes the blood-spinal cord barrier and limits oxidative stress and white matter damage in the acutely injured murine spinal cord. *Journal of Cerebral Blood Flow and Metabolism*, 27(5), 1010-1021.

105. Livak, K. J., and Schimittgen, T. D. (2001). Analysis of relative gene expression data using real-time quantitative PCR and the $2^{-\Delta\Delta C(T)}$ method. *Methods,* 25(4), 402-408.

106. Loboda, A., Jawza, A., Grochot-Przeczek, A., Rutkowski, A. J., Cisowski, J., Agarwal, A., Jozkowicz, A., and Dulak, J. (2008). Heme oxygenase-1 and the

vascular bed: from molecular mechanisms to therapeutic opportunities. *Antioxidants and Redox Signaling,* 10(10), 1767-1812.

107. Lopert, P., and Patel, M. (2014). Nicotinamide nucleotide transhydrogenase (Nnt) links the substrate requirement in brain mitochondria for hydrogen peroxide removal to the thioredoxin/peroxiredoxin (Trx/Prx) system. *Journal of Biological Chemistry*, 289(22), 15611-15620.
108. Lopes da Fonseca, T., Villar-Pique, A., and Outeiro, T. F. (2015). The interplay between alpha-synuclein clearance and spreading. *Biomolecules*, 5(2), 435-471.
109. Luk, K. C., Kehm, V., Carroll, J., Zhang, B., O'Brien, P., Trojanowski, J. Q., and Lee, V. M. Y. (2012). Pathological alpha-synuclein transmission initiates Parkinson-like neurodegeneration in nontransgenic mice. *Science*, 338(6109), 949-953.
110. Lukiw, W. J. (2007). MicroRNA speciation in fetal, adult and Alzheimer's disease hippocampus. *Neuroreport,* 18(3), 297-300.
111. Ma, N., Xiang, Y., Zhang, Y., Zhao, X., Zhou, L., and Gao, X. (2013). The balance mediated by miRNAs and the heme oxygenase 1 feedback loop contributes to biological effects. *Journal of Cellular Biochemistry*, 114, 2637-2642.
112. Marques, O., and Outeiro, T. F. (2012). Alpha-synuclein: from secretion to dysfunction and death. *Cell Death and Disease,* 3(7), e350.
113. Martire, S., Mosca, L., and d'Erme, M. (2015). PARP-1 involvement in neurodegeneration: A focus on Alzheimer's and Parkinson's diseases. *Mechanisms of Ageing and Development,* 146, 53-64.

114. Matz, P., Turner, C., Weinstein, P. R., Massa, S. M., Panter, S. S., and Sharp, F. R. (1996). Heme oxygenase-1 induction in glia throughout rat brain following experimental subarachnoid hemorrhage. *Brain Research,* 713(1), 211-222.

115. Mehindate, K., Sahlas, D. J., Frankel, D., Mawal, Y., Liberman, A., Corcos, J., Dion, S., and Schipper, H. M. (2001). Proinflammatory cytokines promote glial heme oxygenase-1 expression and mitochondrial iron deposition: implications for multiple sclerosis. *Journal of Neurochemistry*, 77(5), 1386-1395.

116. Meiser, J., Weindl, D., and Hiller, K. (2013). Complexity of dopamine metabolism. *Cell Communication and Signaling*, 11(1), 1.

117. Morris, H. R. (2005). Genetics of Parkinson's disease. *Annals of Medicine,* 37(2), 86-96.

118. Morris, P. K., Downes, J. J., Sahakian, B. J., Evenden, J. L., Heald, A., and Robbins, T. W. (1988). Planning and spatial working memory in Parkinson's disease. *Journal of Neurology, Neurosurgery and Psychiatry,* 51(6), 757-766.

119. Nakamura, K., Nemani, V. M., Wallender, E. K., Kaehlcke, K., Ott, M., and Edwards, R. H. (2008). Optical reporters for the conformation of alpha-synuclein reveal a specific interaction with mitochondria. *The Journal of Neuroscience,* 28(47), 12305-12317.

120. Neikrug, A. B., Maglione, J. E., Liu, L., Natarajan, L., Avanzino, J. A., Corey-Bloom, J., Palmer, B. W., Loredo, J. S., and Ancoli-Israel, S. (2013). Effects of sleep disorders on the non-motor symptoms of Parkinson disease. *Journal of Clinical Sleep Medicine,* 9(11), 1119-1129.

121. Ogawa, K. (2002). Heme metabolism in stress response. *Nippon Eiseigaku Zasshi. Japanese Journal of Hygiene,* 56(4), 615-621.

122. Panahian, N., Yoshiura, M., and Maines, M. D. (1999). Overexpression of heme oxygenase-1 is neuroprotective in a model of permanent middle cerebral artery occlusion in transgenic mice. *Journal of Neurochemistry*, 72, 1187-1203.

123. Parent, M., and Parent, A. (2010). Substantia nigra and Parkinson's disease: a brief history of their long and intimate relationship. *Canadian Journal of Neurological Sciences*, 37, 313-319.

124. Parkinson, J. (1817). An essay on the shaking palsy. *The Journal of Neuropsychiatry and Clinical Neurosciences.*

125. Penney, J. B., and Young, A. B. (1986). Striatal inhomogeneities and basal ganglia function. *Movement Disorders Journal,* 1(1), 3-1510.

126. Pizzimenti, S., Ferracin, M., Sabbioni, S., Toaldo, C., Pettazzoni, P., Dianzani, M. U., Negrini, M., and Barrera, G. (2009). MicroRNA expression changes during human leukemic HL-60 cell differentiation induced by 4-hydroxynonenal, a product of lipid peroxidation. *Free Radical Biology and Medicine*, 46, 282-288.

127. Polymeropoulos, M. H., Lavedan, C., Leroy, E., Ide, S. E., Dehejia, A., Dutra, A., Pike, B., Root, H., Rubenstein, J., Boyer, R., Stenroos, E. S., Chandrasekharappa, S., Athanassiadou, A., Papapetropoulos, T., Johnson, W. G., Lazzarini, A. M., Duvoisin, R. C., Di Iorio, G., Golbe, L. I., and Nussbaum, R. L. (1997). Mutation in the alpha-synuclein gene identified in families with Parkinson's disease. *Science*, 276, 2045-2047.

128. Prabakaran, S., Swatton, J. E., Ryan, M. M., Huffaker, S. J., Huang, J. T., Griffin, J. L., Wayland, M., Freeman, T., Dudbridge, F., Lilley, K. S., Karp, N. A., Hester, S., Tkachev, D., Mimmack, M. L., Yolken, R. H., Webster, M. J., Torrey, E. F., and Bahn, S. (2004). Mitochondrial dysfunction in schizophrenia: evidence for compromised brain metabolism and oxidative stress. *Molecular Psychiatry,* 9(7), 684-697.

129. Preisig-Muller, R., y Schnitzler, M. M., Derst, C., and Daut, J. (1999). Separation of cardiomyocytes and coronary endothelial cells for cell-specific RT-PCR. *American Journal of Physiology – Heart and Circulatory Physiology,* 277(1), H413-H416.

130. Qato, M. K., and Maines, M. D. (1985). Prevention of neonatal hyperbilirubinaemia in non-human primates by Zn-protoporphyrin. *Biochemical Journal*, 226(1), 51-57.

131. Rousseaux, M. W., Marcogliese, P. C., Qu, D., Hewitt, S. J., Seang, S., Kim, R. H., Slack, R. S., Schlossmacher, M. G., Lagace, D. C., Mak, T. W., and Park, D. S. (2012). Progressive dopaminergic cell loss with unilateral-to-bilateral progression in a genetic model of Parkinson disease. *Proceedings of the National Academy of Sciences,* 109(39), 15918-15923.

132. Ryter, S. W., and Tyrrell, R. M. (2000). The heme synthesis and degradation pathways: Role in oxidant sensitivity: Heme oxygenase has both pro- and antioxidant properties. *Free Radical Biology and Medicine,* 28(2), 289-309.

133. Sacino, A. N., Brooks, M., McKinney, A. B., Thomas, M. A., Shaw, G., Golde, T. E., and Giasson, B. I. (2014). Brain injection of alpha-synuclein induces multiple

proteinopathies, gliosis, and a neuronal injury marker. *The Journal of Neuroscience*, 34, 12368-12378.

134. Saggu, H., Cooksey, J., Dexter, D., Wells, F. R., Lees, A., Jenner, P., and Marsden, C. D. (1989). A selective increase in particulate superoxide dismutase activity in parkinsonian substantia nigra. *Journal of Neurochemistry*, 53(3), 692-697.

135. Samii, A., Nutt, J. G., and Fansom, B. R. (2004). Parkinson's disease. *The Lancet,* 363(9423), 1783-1793.

136. Schapira, A. H., Cooper, J. M., Dexter, D., Jenner, P., Clark, J. B., and Marsden, C. D. (1989). Mitochondrial complex I deficiency in Parkinson's disease. *Journal of Neurochemistry,* 54(3), 823-827.

137. Schenck, C. H., Bundle, S. R., and Mahowald, M. W. (1996). Delayed emergence of a parkinsonian disorder in 38% of 29 older men initially diagnosed with idiopathic rapid eye movement sleep behaviour disorder. *Neurology,* 46(2), 388-393.

138. Schickel, R., Park, S. M., Murmann, A. E., and Peter, M. E. (2010). MiR-200c regulates induction of apoptosis through CD95 by targeting FAP-1. *Molecular Cell*, 38(6), 908-915.

139. Schipper, H. M. (2000). Heme oxygenase-1: role in brain aging and neurodegeneration. *Experimental Gerontology,* 35(6), 821-830.

140. Schipper, H. M. (2004). Brain iron deposition and the free radical-mitochondrial theory of ageing. *Ageing Research Reviews,* 3(3), 265-301.

141. Schipper, H. M. (2007). Biomarker potential of heme oxygenase-1 in Alzheimer disease and mild cognitive impairment. *Biomarkers in Medecine,* 1(3), 375-385.

142. Schipper, H. M. (2015). Is glial heme oxygenase-1 suppression in neurodegenerative disorders permissive for neural repair? *Neural Regeneration Research*, 10(2), 208-210.

143. Schipper, H. M., and Song W. (2015). A heme oxygenase-1 transducer model of degenerative and developmental brain disorders. *International Journal of Molecular Science*, 16, 5400-5419.

144. Schipper, H. M., Cisse, S., and Stopa, E. G. (1995). Expression of heme oxygenase-1 in the senescent and Alzheimer-diseased brain. *Annals in Neurology*, 37(6), 758-768.

145. Schipper, H. M., Liberman, A., and Stopa, E. G. (1998). Neural heme oxygenase-1 expression in idiopathic Parkinson's disease. *Experimental Neurology,* 150(1), 60-68.

146. Schmidt, N., and Ferger, B. (2001). Neurochemical findings in the MPTP model of Parkinson's disease. *Journal of Neural Transmission*, 108, 1263-1282.

147. Sethi, P., and Lukiw, W. J. (2009). MicroRNA abundance and stability in human brain: specific alterations in Alzheimer's disease temporal lobe neocortex. *Neuroscience Letters,* 459(2), 100-104.

148. Shavali, S., Brown-Borg, H. M., Ebadi, M., and Porter, J. (2008). Mitochondrial localization of alpha-synuclein protein in alpha-synuclein overexpressing cells. *Neuroscience Letters,* 439(2), 125-128.

149. Shulman, L. M., Taback, R. L., Bean, J., and Weiner, W. J. (2001). Comorbidity of the nonmotor symptoms of Parkinson's disease. *Movement Disorders,* 16(3), 507-510.

150. Shults, C. W., Haas, R. H., Passov, D., and Beal, M. F. (1997). Coenzyme Q10 levels correlate with the activities of complexes I and II/III in mitochondria from parkinsonian and nonparkinsonian subjects. *Annals of Neurology,* 42(2), 261-264.

151. Siderowf, A., Jennings, D., Connolly, J., Doty, R. L., Marek, K., and Stern, M. B. (2007). Risk factors for Parkinson's disease and impaired olfaction in relatives of patients with Parkinson's disease. *Movement Disorders,* 22(15), 2249-2255.

152. Simone, N. L., Soule, B. P., Ly, D., Saleh, A. D., Savage, J. E., Degraff, W., Cook, J., Harris, C. C., Gius, D., and Mitchell, J. B. (2009). Ionizing radiation-induced oxidative stress alters miRNA expression. *PLoS One*, 4, e6377.

153. Smith, K. M., and Dahodwala, N. (2014). Sex differences in Parkinson's disease and other movement disorders. *Experimental Neurology,* 259, 44-56.

154. Somel, M., Guo, S., Fu, N., Yan, Z., Hu, H. Y., Xu, Y., Yuan, Y., Ning, Z., Hu, Y., Menzel, C., Hu, H., Lachmann, M., Zeng, R., Chen, W., and Khaitovich, P. (2010). MicroRNA, mRNA, and protein expression link development and aging in human macaque brain. *Genome Research*, 20(9), 1207-1218.

155. Song, L., Song, W., and Schipper, H. M. (2007). Astroglia overexpressing heme oxygenase-1 predispose co-cultured PC12 cells to oxidative injury. *The Journal of Neuroscience Research*, 85, 2186-2195.

156. Song, W., Liberman, A., and Schipper, H. M. (2013). Parkinsonian features in aging GFAP.HMOX1 transgenic mice overexpressing human HO-1 in the astroglial compartment. *Journal of Parkinson's Disease,* 3(1), 69.

157. Song, W., Patel, A., Qureshi, H. Y., Han, D., Schipper, H. M., and Paudel, H. K. (2009). The Parkinson disease-associated A30P mutation stabilizes alpha-synuclein against proteasomal degradation triggered by heme oxygenase-1 over-expression in human neuroblastoma cells. *Journal of Neurochemistry,* 110(2), 719-733.

158. Song, W., Zukor, H., Lin, S. H., Hascalovici, J., Liberman, A., Tavitian, A., Mui, J., Vali, H., Tong, X. K., Bhardwaj, S. K., Srivastava, L. K., Hamel, E., and Schipper, H. M. (2012). Schizophrenia-like features in transgenic mice overexpressing human HO-1 in the astrocytic compartment. *The Journal of Neuroscience,* 32(32), 10841-10853.

159. Stary, C. M., Xu, L., Sun, X., Ouyang, Y. B., White, R. E., Leong, J., Li, J., Xiong, X., Giffard, R. G. (2015). MicroRNA-200c contributes to injury from transient focal cerebral ischemia by targeting Reelin. *Stroke*, 46(2), 551-556.

160. Storm, T., Rath, S., Mohamed, S. A., Bruse, P., Kowald, A., Oehmichen, M., and Meissner, C. (2002). Mitotic brain cells are just as prone to mitochondrial deletions as neurons: A large-scale single-cell PCR study of the human caudate nucleus. *Experimental Gerontology*, 37, 1389-1400.

161. Subramaniam, M., Althof, D., Gispert, S., Schwenk, J., Auburger, G., Kulik, A., Fakler, B., and Roeper, J. (2014). Mutant alpha-synuclein enhances firing

frequencies in dopamine substantia nigra neurons by oxidative impairment of A-type potassium channels. *The Journal of Neuroscience,* 34(41), 13586-13599.

162. Sun, J., Hoshino, H., Takaku, K., Nakajima, O., Muto, A., Suzuki, H., Tashiro, S., Takahashi, S., Shibahara, S., Alam, J., Taketo, M. M., Yamamototo, M., and Igarashi, K. (2002). Hemoprotein Bach1 regulates enhancer availability of heme oxygenase-1 gene. *The EMBO Journal,* 21(19), 5216-5224.

163. Suzuki, H., Tashiro, S., Sun, J., Doi, H., Satomi, S., Igarashi, K. (2003). Cadmium induces nuclear export of Bach1, a transcriptional repressor of heme oxygenase-1 gene. *Journal of Biological Chemistry,* 278(49), 49246-49253.

164. Sydow, A., Van der Jeugd, A., Zheng, F., Ahmed, T., Balschun, D., Petrova, O., Drexler, D., Zhou, L., Rune, G., Mandelkow, E., D'Hooge, R., Alzheimer, C., and Mandelkow, E. M. (2011). Reversibility of Tau-related cognitive defects in a regulatable FTD mouse model. *Journal of Molecular Neuroscience*, 45, 432-437.

165. Takeda, A., Perry, G., Abraham, N. G., Dwyer, B. E., Kutty, R. K., Laitnen, J. T., Petersen, R. B., and Smith, M. A. (2000). Overexpression of heme oxygenase in neuronal cells, the possible interaction with Tau. *Journal of Biological Chemistry*, 275, 5395-5399.

166. Tandberg, E., Larsen, J. P., and Karlsen, K. (1998). A community-based study of sleep disorders in patients with Parkinson's disease. *Movement Disorders,* 13(6), 895-900.

167. Tapia-Gonzalez, S., Giraldez-Perez, R. M., Cuartero, M. I., Cassarejos, M. J., Mena, M. A., Wang, X. F., and Sanchez-Capelo, A. (2011). Dopamine and alpha-synuclein dysfunction in Smad3 null mice. *Molecular Neurodegeneration*, 6, 72.

168. Tatton, N. A. (2000). Increased caspase 3 and Bax immunoreactivity accompany nuclear GAPDH translocation and neuronal apoptosis in Parkinson's disease. *Experimental Neurology*, 166(1), 29-43.

169. Tatton, W. G., Chalmers-Redman, R., Brown, D., and Tatton, N. (2003). Apoptosis in Parkinson's disease: signals for neuronal degradation. *Annals of Neurology*, 53(S3), S61-S72.

170. Tekirdag, K. A., Korkmaz, G., Ozturk, D. G., Agami, R., and Gozuacik, D. (2013). MIR181A regulates starvation- and rapamycin-induced autophagy through targeting of ATG5. *Autophagy*, 9, 374-385.

171. Van Rooj, E., Sutherland, L. B., Qi, X., Richardson, J. A., Hill, J., and Olson, E. N. (2007). Control of stress-dependent cardiac growth and gene expression by a microRNA. *Science*, 316(5824), 575-579.

172. Vaya, J., Song, W., Khatib, S., Geng, G., and Schipper, H. M. (2007). Effects of heme oxygenase-1 expression on sterol homeostasis in rat astroglia. *Free Radical Biology and Medicine,* 42(6), 864-871.

173. Vincent, S. R., Das, S., and Maines, M. D. (1994). Brain heme oxygenase isoenzymes and nitric oxide synthase are co-localized in select neurons. *Neuroscience,* 63(1), 223-231.

174. Wagner-Ecker, M., Schwager, C., Wirkner, U., Abdollahi, A., and Huber, P. E. (2010). MicroRNA expression after ionizing radiation in human endothelial cells. *Radiation Oncology*, 5, 25.

175. Wang, L., Huang, H., Fan, Y., Kong, B., Hu, H., Hu, K., Guo, J., Mei, Y., and Liu, W. L. (2014). Effects of downregulation of microRNA-181a on H2O2-induced H9c2

cell apoptosis via the mitochondrial apoptotic pathway. *Oxidative Medicine and Cellular Longevity*, 2014, 960362.

176. Wang, W. X., Visavadiya, N. P., Pandya, J. D., Nelson, P. T., Sullivan, P. G., and Springer, J. E. (2015). Mitochondria-associated microRNAs in rat hippocampus following traumatic brain injury. *Experimental Neurology,* 265, 84-93.

177. Westerlund, M., Hoffer, B., and Olson, L. (2010). Parkinson's disease: Exit toxins, enter genetics. *Progress in Neurobiology,* 90(2), 146-156.

178. Winklhofer, K. F., Tatzelt, J., and Haass, C. (2008). The two faces of protein misfolding: gain- and loss-of-function in neurodegenerative diseases. *The EMBO Journal,* 27(2), 336-349.

179. Yamamoto, A., Lucas, J. J., and Hen, R. (2000). Reversal of neuropathology and motor dysfunction in a conditional model of Huntington's disease. *Cell*, 101, 57-66.

180. Yonetani, M., Nonaka, T., Masuda, M., Inukai, Y., Oikawa, T., Hisanaga, S. I., and Hasegawa, M. (2009). Conversion of wild-type alpha-synuclein into mutant-type fibrils and its propagation in the presence of A30P mutant. *Journal of Biological Chemistry*, 284(12), 7940-7950.

181. Yoritaka, A., Hattori, N., Uchida, K., Tanaka, M., Stadtman, E., and Mizuno, Y. (1996). Immunohistochemical detection of 4-hydroxynonenal protein adducts in Parkinson disease. *Proceedings of the National Academy of Sciences,* 93(7), 2696-2701.

182. Zhang, J., Perry, G., Smith, M. A., Robertson, D., Olsen, S. J., Graham, D. G., and Montine, T. J. (1999). Parkinson's disease is associated with oxidative

damage to cytoplasmic DNA and RNA in substantia nigra neurons. *The American Journal of Pathology,* 154(5), 1423-1429.

183. Zhang, L., Zhang, C., Zhu, Y., Cai, Q., Chan, P., Ueda, K., Yu, S., and Yang, H. (2008). Semi-quantitative analysis of alpha-synuclein in subcellular pools of rat brain neurons: An immunogold electron microscopic study using a C-terminal specific monoclonal antibody. *Brain Research,* 1244, 40-52.

184. Zukor, H., Song, W., Liberman, A., Mui, K., Vali, H., Fillebeen, C., Pantopoulos, K., Wu, T. D., Guerquin-Kern, J. L., and Schipper, H. M. (2009). HO-1-mediated macroautophagy: a mechanism for unregulated iron deposition in aging and degenerating neural tissues. *Journal of Neurochemistry,* 109(3), 776-791.